THESIS REPORT
Master's Degree

Institute for Systems Research

Intelligent Process Control

by N.S. Patel
Advisor: J.S. Baras

The Institute for Systems Research is supported by the National Science Foundation Engineering Research Center Program (NSFD CD 8803012), Industry and the University

M.S. 93-4

Abstract

Title of thesis: Intelligent Process Control

Name of degree candidate: Nital S. Patel

Degree and year: Master of Science in Electrical Engineering, 1993

Thesis directed by: John S. Baras
Professor
Electrical Engineering

It is often observed that human experts can tune the parameters of a controller based on their knowledge and experience, rather than on complicated algorithms. In fact, more often than not, they have only a vague idea of the process model. An attempt is made here to create a fuzzy-logic based expert which would emulate such behaviour. The expert is, specifically designed to tune the gains of a Proportional-Integral-Derivative (PID) controller, applied to stable dominant pole plants having large rise times. It is observed, that a number of plants found in the chemical process industry can be suitably modeled as such systems. A rule base for the expert was developed after analysis and simulation studies. Attempts have been made to keep the rules as few and simple as possible. At no point is any attempt made to estimate the parameters of the plant model. The expert observes only the output from the plant. Results of the application of the expert

to a second order plant, to the separator temperature control loop of the Tennessee Eastman problem, and to a third order plant are presented. The expert is found to successfully tune the PID gains, and the results provide encouragement for the creation of such experts which can handle a class of plants.

INTELLIGENT PROCESS CONTROL

by

Nital S. Patel

Thesis submitted to the Faculty of the Graduate School
of The University of Maryland in partial fulfillment
of the requirements for the degree of
Master of Science
1993

Advisory Committee:

Professor John S. Baras, Chairman/Advisor
Professor P.S. Krishnaprasad
Professor Thomas J. McAvoy

DEDICATION

To my parents

ACKNOWLEDGEMENTS

I would like to express my sincere appreciation to my advisor Dr. J. S. Baras for his guidance and encouragement on my graduate research. His ideas and suggestions on intelligent control made my work all the more stimulating. I would also like to thank Dr. Evanghelos Zafiriou for his comments on open-loop stability and industrial practices in the chemical process industry. I owe additional thanks to Dr. Krishnaprasad, and Dr. McAvoy for serving on my thesis advisory committee.

I am grateful to my colleagues in the Systems Integration Laboratory for making the lab a great place to work. Thanks also to Tina Vigil for maintaining a steady supply of candies.

Finally, I would like to thank the Institute for Systems Research for my fellowship support.

This research was supported by the National Science Foundation Engineering Research Centers Program: NSFD CDR 8803012.

Contents

List of Figures

List of Tables

Chapter 1

Introduction

The recent stimulus for the application of Intelligent Control systems to the chemical process industry has resulted in the proposal of a variety of schemes. However, most of these are targeted toward specific applications. The need is to develop algorithms for Intelligent Control that are applicable to a broader class of problems [Åström and McAvoy, 1992].

It is often seen that control experts tune the parameters of a controller according to error verses time curves based on their knowledge and experience, rather than on complicated algorithms (the latter mean complicated calculations, which makes it very difficult to control a process effectively and successfully). In fact, when a process is controlled, there are interior relations between the shapes of a control curve and the parameters of a controller, which are an important basis for the tuning action of a control expert. This kind of tuning method, if realizable is captivating because it does not require an accurate process model, which is generally unavailable in practice. Hence, an *expert* developed with such a principle in mind will be intelligent and universal to various controlled processes. This thesis describes the development of such an expert for processes which can be modelled approximately as second order systems. This expert tunes the parameters of a Proportional-Integral-Derivative (PID) controller which is being used in the feedback loop to control the process. The tuning strategy is based on a comparison of the response and error curves generated by the plant to a desired *good* response. It should be mentioned here that the response obtained cannot be called optimal in any given sense. The fact that this strategy, is applicable to cases where the plant model is never precisely known precludes any notion of optimality. Rather, what is desired here is that the response be acceptable in some sense. It should be noted here, that this tuning strategy deviates from the current trend, where effort is made to obtain information about the plant by carrying out data analysis and modeling. A review of these techniques can be found in [Koivo and Tanttu, 1991].

A major effort of this thesis is the derivation of the fuzzy relational equations which are used to represent the tuning strategy. Since no purely second order process exists in practice, it is not possible to obtain these relational equations by emulating a human expert. Rather, they have been constructed after extensive root locus studies and simulations. All efforts have been made to keep these equations as few in number, and as simple as possible, so that they may give some insight into their behaviour, and lend themselves to some kind of mathematical analysis (though further work is required on the latter due to the lack of mathematical tools to handle fuzzy quantities). An order of magnitude analysis presented shows that these rules indeed function as required. The latter is another effort of this thesis, since most fuzzy control applications found in the literature ignore such analysis.

Chapter 2 of this thesis states the problem and the approach used to arrive at the solution. The validity of choosing this class of second order systems is addressed. Justification is provided for the use of fuzzy logic. Also addressed is the question of using fuzzy control for parameter tuning, rather than for direct control.

Chapter 3 deals with the derivation of the fuzzy relational equations. Starting with initial actions based on damping and the natural frequency, the required movement of the closed loop poles is illustrated. The idea of moving these poles by manipulating the PID controller zeroes is then discussed. At the conclusion of the chapter, the fuzzy relational equations are presented.

Chapter 4 deals with the implementation of the expert. The definition of the fuzzy membership functions for the various measured and manipulated variables is discussed. The method used to combine the output classes to get a numerical quantity is presented. The advantage of scaling the outputs for different PID controller gains is illustrated, especially in lieu of the order of magnitude analysis.

The application of this expert is the content of Chapter 5. Three applications are discussed. Firstly to a known second order system, and secondly to the separator temperature control in the Tennessee Eastman test problem, and thirdly to a third order plant.

Conclusions are discussed in Chapter 6. Also included are suggestions for future work. The importance of the need of mathematical methods to handle fuzzy quantities is reiterated.

Appendix A gives a discussion on the influence of the PID zeroes on the closed loop poles when the plant is of second order.

The Appendix B gives an order of magnitude analysis which is used to verify the validity of the fuzzy relational equations under specific assumptions.

It should be noted that the expert has to satisfy at least two performance criteria. 1) As with humans, satisfactory learning requires frequent repetition of the same effort, so the system is improved by being restarted from the same initial conditions again and again. 2) Important for technical control problems is the ability to stabilize the control loop in the first trial, however, with relatively bad performance in general.

Chapter 2

Overview of the Problem

2.1 Statement of the Problem

By large, chemical plants comprise of components designed to exhibit open loop stability. It has been recognized long ago [Oldenburg and Sartorius, 1948] that most systems can be represented by a second order system together with a delay as

$$\frac{Y(s)}{E(s)} = \frac{Ke^{-st_D}}{(\tau_1 s + 1)(\tau_2 s + 1)} \tag{2.1}$$

where $Y(s)$ = Output Signal

$E(s)$ = Input Signal

K = Process Gain

t_D = Dead Time (Delay)

τ_1, τ_2 = Process Time Constants

An extensive bibliography of the different chemical processes that have been approximated successfully by this model is given in [Latour *et al.*, 1967], and [Bohl and McAvoy, 1976]. The interest here is in systems which have $\tau_1 \gg \tau_2$ i.e. the response is dominated by a single mode. It is also assumed for the moment that the dead time does not have a significant influence on the dynamic behaviour of the system. This is elaborated upon in Chapter 3, where the influence of dead times on the root locus is examined. For the moment the dead time is neglected.

Hence given a second order plant

$$P(s) = \frac{Y(s)}{E(s)} = \frac{K}{(\tau_1 s + 1)(\tau_2 s + 1)} \tag{2.2}$$

where $\tau_1 \gg \tau_2$, along with a PID controller

$$C(s) = \frac{R(s)}{Y(s)} = K_C + \frac{K_I}{s} + K_D s \tag{2.3}$$

configured as in Figure 2.1, the aim is to develop a strategy to tune K_C,K_I and K_D so as to get a *good* response to setpoint changes $S(s)$. This concept of a good response is explained in Section 4.1.

An important factor to be considered here is the amount of information required about the plant $P(s)$. It is assumed that the only information available is the approximate response time to changes in $E(s)$, and an estimate of the dead time if any. Such information is easily available from designers or an expert.

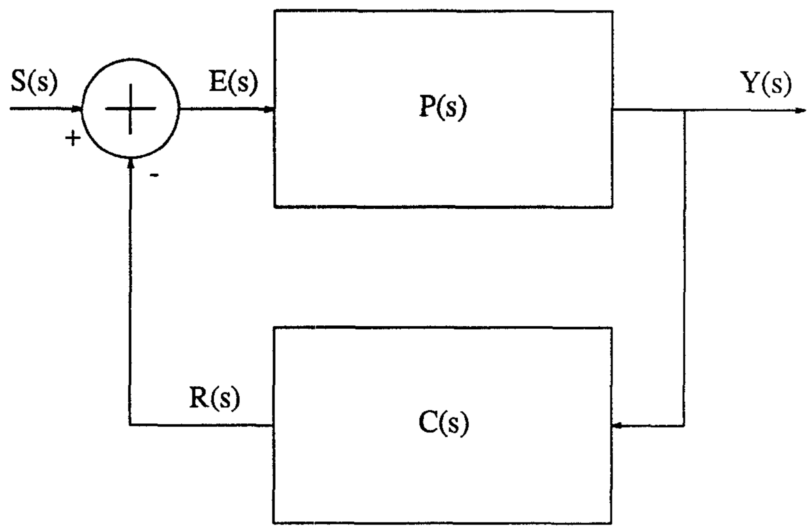

Figure 2.1: Plant-Controller Configuration

2.2 Fuzzy Control

Due to the general nature of the problem, the solution if any, may be expected to be numerically complex. Since the plant itself is not precisely specified (i.e. τ_1,τ_2 and K are unknown), and no attempt is made to identify it, not much mileage is expected out of conventional approaches. On the other hand such a problem is an ideal candidate for fuzzy logic-based control. A good introduction to fuzzy logic can be found in [Self, 1990]. For a more thorough treatment, the reader is referred to [Pedrycz, 1989]. Interest in fuzzy control has increased recently because of good practical experiences in the control of cement kilns [Holmblad and Østergaard, 1981], and other areas, and the creation of the institute of fuzzy control in Japan [Sugeno, 1985], [van der Rhee *et al.*, 1990].

Fuzzy logic-based control has been observed to have excellent robustness char-

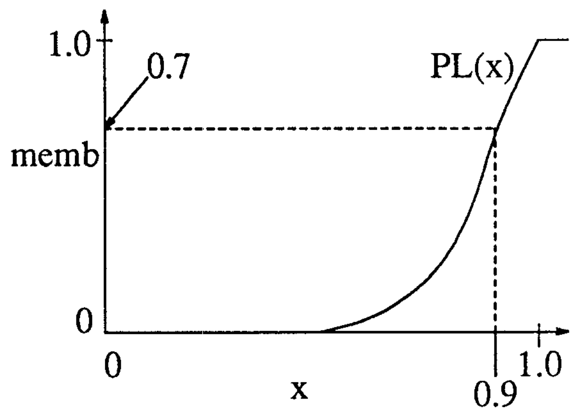

Figure 2.2: Fuzzy Membership Function

acteristics [Bernard, 1988], perhaps because the inherent imprecision, or generality of the fuzzy decision rules is well suited to imprecise systems whose behaviour is known only in the large. Hence, fuzzy control systems are able to achieve satisfactory, stable behaviour, albeit a non-optimal one over wide fluctuations in system parameter values [Chiu *et al.*, 1990].

At the basis of such a controller is the concept of *membership functions* [Zadeh, 1973]. These are used to generate linguistic descriptions. These membership functions indicate the degree to which a value belongs to the class labeled by the linguistic description. For example, the linguistic description *Positive Large* maybe represented by the membership function PL(x) shown in Figure 2.2, where the abscissa is a measured input and the ordinate is the degree to which the input value can be classified as Positive Large. In this example, the degree to which 0.9 is considered to be Positive Large is 0.7, i.e. PL(0.9) = 0.7.

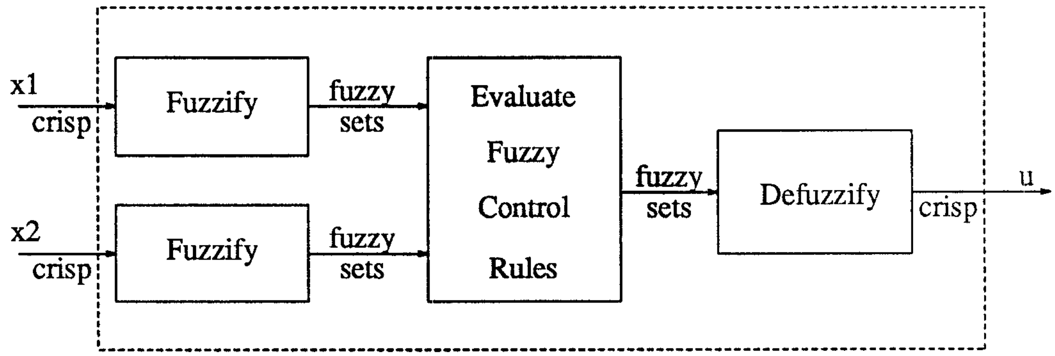

Figure 2.3: Fuzzy Controller Schematic

Fuzzy control rules are typically expressed in the following form:

$$If\ X_1\ is\ A_{i,1}\ and\ X_2\ is\ A_{i,2}\ then\ U\ is\ B_i \tag{2.4}$$

where X_1 and X_2 are the inputs to the controller, U is the output, A's and B's are membership functions, and the subscript i denotes the rule number. For example, a rule for engine speed control may state *If speed error is negative small and the change in speed error is positive large, then the change in throttle is positive small.* Given input values X_1 and X_2, the *degree of fulfillment* (DOF) of rule i is given by the minimun of the degree of satisfaction of the individual antecedent clauses. i.e.

$$DOF_i = min\{A_{i,1}(X_1), A_{i,2}(X_2)\} \tag{2.5}$$

The output value is computed by

$$u = \frac{\sum_{i=1}^{n}(DOF_i)B_i^d}{\sum_{i=1}^{n}(DOF_i)} \tag{2.6}$$

where B_i^d is the *defuzzified* value of the membership function B_i, and n is the number of rules. The defuzzified value of a membership function is the single value that best represents the linguistic description. Typically the abscissa of the centroid of a membership function is taken as the defuzzified value.

In essence, each rule contributes a conclusion weighed by the degree to which the antecedent of the rule is fulfilled. The final control decision is obtained as the weighed average of all the contributed conclusions.

A schematic of a fuzzy controller is shown in Figure 2.3. The evaluation of fuzzy rules can be done either sequentially, or in parallel using a Fuzzy Associative Memory (FAM) to store the rules [Kosko, 1990].

2.3 System Architecture

The intent here is to tune the gains of a PID controller, so as to push the closed loop response towards a desired response. The measurements available are 1) the plant output $y(t)$, and 2) the setpoint s, which is assumed to be constant for the period of the response. Based on these measurements, the overall system level architecture is as shown in Figure 2.4. It should be observed that there are two objectives to be satisfied.

1. To ensure that the rise time of the response is as close to the specified value as possible.

2. The settling time is small.

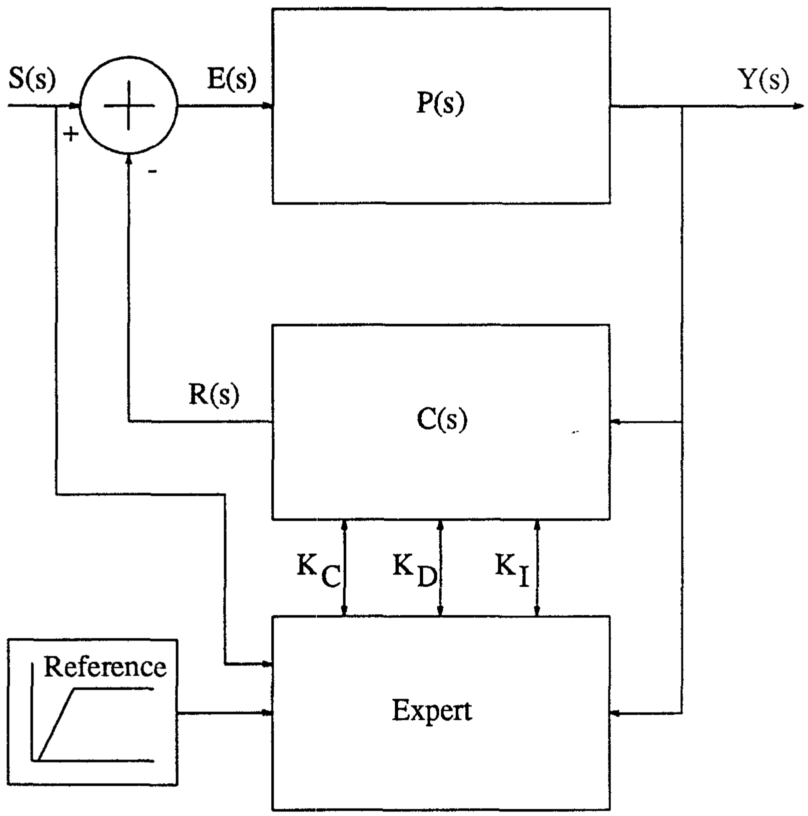

Figure 2.4: Overall System Architecture

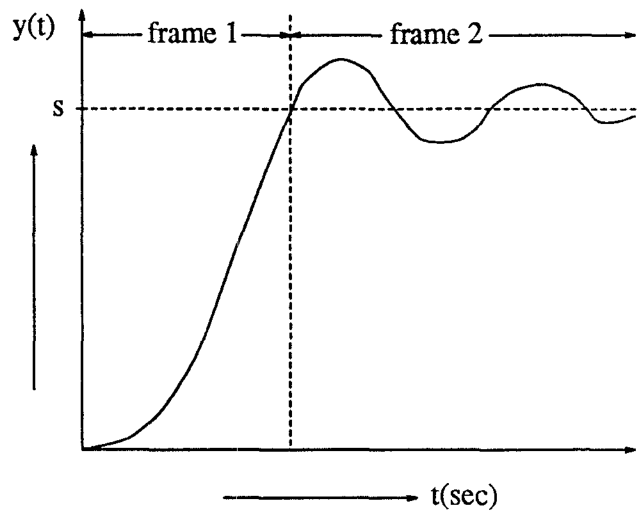

Figure 2.5: Division of the Response into Frames

The rise time is specified through the *good* response curve. There is however no provision for specifying the settling time, although the expert tends to make it reasonably small. Both these requirements are kind of contradictory since a short rise time will result in more oscillations about the steady state due to lower damping. Also due to the nature of the measurements, it is seen that two sets of rules are required, and the actions of the expert are different in the two regimes of the response. Hence the response is divided into two *frames* . The response is in frame 1 till it first reaches the set point, and in frame 2 thereafter. This is illustrated in Figure 2.5. The damping requirements, and the rule bases for these two regimes is the subject of Chapter 3.

Justification is needed to explain the use of fuzzy logic for indirect control rather than direct control. If fuzzy control is robust then why not use it directly in the feedback loop, instead of using it to tune the parameters of a PID controller ?

This is explained by the fact that due to the nature of its generality, fuzzy control is inherently imprecise and if used directly in the feedback loop, would introduce error into the control signal. Hence a PID controller is retained since it is not prone to such imprecision and the response characteristics are controlled through the fuzzy controller by tuning the PID gains.

Chapter 3

Derivation of Fuzzy Rules

3.1 Specifications and Measurements

The reference response is specified by two parameters T_1 and T_2. T_1 specifies a dead time, i.e. it is the time taken by the system to start responding, and T_2 specifies the time taken by the system to reach the set-point value from zero for the first time. This response curve is illustrated in Figure 3.1. Hence all one needs to determine is, what dead time and rise time values are required for the particular case at hand. Conservative estimates of these can be obtained from the plant designer, or an expert. The steady state value of the reference response always equals 1.

For the purposes of tuning the parameters of the PID controller, the set-point (s), and the plant output ($y(t)$) are measured. While the response is in frame 1

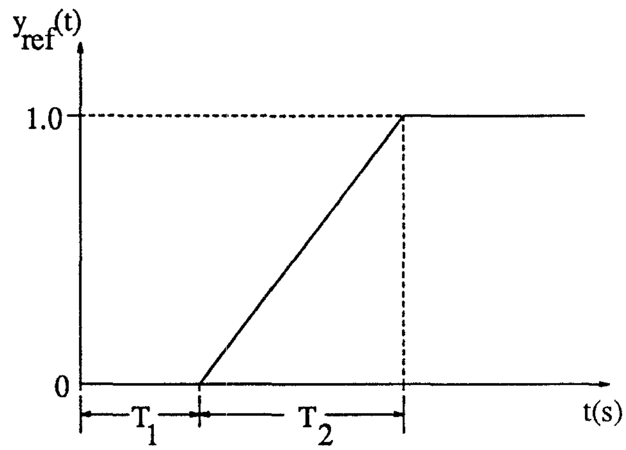

Figure 3.1: Reference Response

(see Figure 2.5) the plant output is scaled as

$$y\prime(t) = \frac{y(t) - s_{old}}{s_{new} - s_{old}} \tag{3.1}$$

where s_{new} is the new set-point and s_{old} is the previous set-point. This scales the output, and $y\prime(t)$ lies in the range between 0 and 1. The error fed to the expert is then calculated as

$$e_1(t) = y_{ref}(t) - y\prime(t) \tag{3.2}$$

where $y_{ref}(t)$ is the value of the reference response specified as explained above, and the subscript 1 in $e_1(t)$ refers to frame 1.

For frame 2 the error $e_2(t)$ is calculated directly as

$$e_2(t) = s_{new} - y(t) \tag{3.3}$$

where the subscript 2 refers to frame 2. The reason for not scaling the error in this frame is that irrespective of the magnitude of the set-point change, the measurement noise remains the same, and hence scaling especially for a small set-point change could result in erroneous behaviour. Once $e_2(t)$ is known, its derivative $\frac{de_2(t)}{dt}$ can be calculated.

3.2 Action in Frame 2

A special note needs to be made about how the expert is made to handle frame 2. Consider a typical response as shown in Figure 3.2. The response is in frame 1 till it reaches the set-point (s) value for the first time. Since the plant model is not known, there is no way to judge the response as being unstable, underdamped but stable, or perfectly damped. Too much damping applied at this point may delay the return of the response back to steady state. On the other hand, reduction of damping may result in large oscillations. So at this point in time, the expert does nothing except wait for the response to reach point 2 i.e. at the peak of the overshoot/undershoot.

Once point 2 is reached and the response starts returning to the steady state value, action is taken by the expert. Hence in frame 2 the expert acts only when the response is returning to the steady state value (i.e. between points 2 and 3, 4 and 5 etc.).

One may argue that since the plant is assumed to be approximately second order, one may use the wealth of formulae available for analyzing underdamped

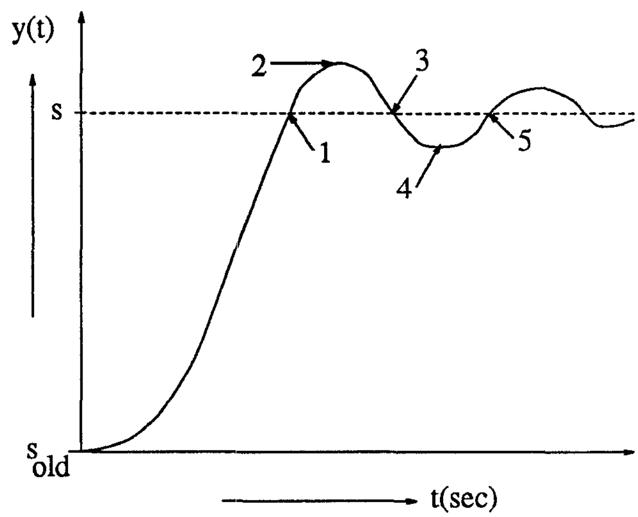

Figure 3.2: A Typical Response

second order systems. It is trivial to see that due to the integral mode in the controller, the system is actually of order 3, and since the plant poles are not known one cannot carry out order reduction.

3.3 Response and Damping

To tune the closed-loop response to approximate the desired response, the damping ratio (ξ) and the natural frequency (ω) have to be manipulated. The relationship between these and the poles of the closed-loop system are illustrated in Figure 3.3.

It is worthwile to stop here and review the influence of ξ and ω on the rise time (t_r) and settling time (t_s) of a second order system. The following equations [Kuo, 1991] hold for a pure second order system in response to a step change in

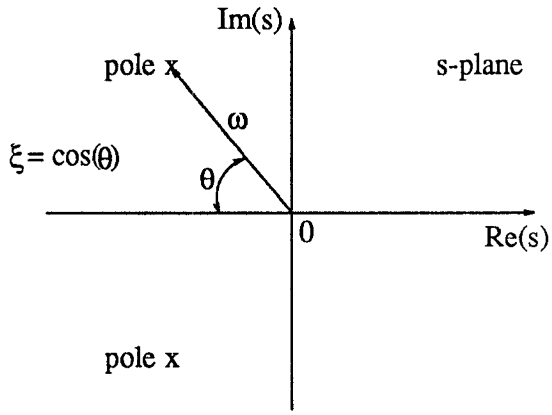

Figure 3.3: Poles, Damping (ξ), and Natural Frequency (ω)

the set-point.

$$t_r \approx \frac{0.8 + 2.5\xi}{\omega} \qquad ,0 < \xi < 1 \tag{3.4}$$

$$t_s = -\frac{1}{\xi\omega}\ln(0.05\sqrt{1-\xi^2}) \qquad ,0 < \xi < 1 \tag{3.5}$$

where t_s is the time taken by the response to reach within $\pm 5\%$ of the steady state value, and remain within this bound for all future time.

Although systems in practice are never going to be purely second order, the above helps in a qualitative description of the dependencies between the various variables. Hence to decrease the rise time (t_r) one needs to decrease ξ or increase ω or do both. Also to decrease the settling time (t_s) one needs to increase ξ or increase ω or do both.

The inputs to the fuzzy controller $e_1(t)$, $e_2(t)$, and $\frac{de_2(t)}{dt}$ are each divided into seven fuzzy classes. Namely: 1) Positive Large (PL), 2) Positive Medium (PM), 3) Positive Small (PS), 4) Zero (Z), 5) Negative Small (NS), 6) Negative Medium (NM), and 7) Negative Large (NL).

For frame 1 only $e_1(t)$ is measured. If the current closed loop response is slower than the reference response, then $e_1(t)$ is positive. To compensate for this, the damping ratio should be decreased and/or the natural frequency increased i.e. the closed loop poles are moved towards the imaginary axis, and/or away from the real axis, the latter by a greater amount. The larger the error ($e_1(t)$), the larger the movement of the poles. If on the other hand, the response is faster than the desired reference response, then $e_1(t)$ is negative and the damping ratio is increased, and/or the natural frequency decreased i.e. the closed loop poles are moved away from the imaginary axis, and/or towards the real axis, the latter by a greater amount.

In frame 2 both the error ($e_2(t)$), and the rate of change of error ($\frac{de_2(t)}{dt}$) are used to characterize the response. If $e_2(t)$ is not *small* , and if $\frac{de_2(t)}{dt}$ is not *zero* , the damping factor is increased and the natural frequency increased by an amount determined by the fuzzy membership of both $e_2(t)$ and $\frac{de_2(t)}{dt}$. If however $e_2(t)$ is *small* and $\frac{de_2(t)}{dt}$ is *zero* then the damping factor is decreased to enable the response to return to steady state as quickly as possible.

The variation in controller gains required to achieve this is discussed after some more discussion based on the root locus technique is presented.

3.4 Analysis Based on the Root Locus Technique

The root locus technique is useful in a qualitative discussion on the influence of higher order poles, and the relationship between the closed-loop poles and the controller zeroes.

Given a closed loop system

$$G(s) = \frac{P(s)}{1 + C(s)P(s)} \tag{3.6}$$

the roots of the characteristic equation must satisfy

$$1 + C(s)P(s) = 0 \quad . \tag{3.7}$$

Suppose that $C(s)P(s)$ contains a variable parameter N as a factor, such that

$$C(s)P(s) = NC_1(s)P_1(s) \tag{3.8}$$

then the characteristic equation can be written as

$$1 + NC_1(s)P_1(s) = 0 \tag{3.9}$$

$$\Rightarrow \quad C_1(s)P_1(s) = -\frac{1}{N} \quad . \tag{3.10}$$

To satisfy the last equation for $N \geq 0$, the following two conditions must be met simultaneously.

$$\mid C_1(s)P_1(s) \mid = \frac{1}{\mid N \mid} \qquad , N \geq 0 \tag{3.11}$$

and

$$\angle C_1(s)P_1(s) = (2k+1)\pi \qquad , N \geq 0 \tag{3.12}$$

where $k = 0, \pm 1, \pm 2, \ldots$

Of all the properties of the root locus, the following ones are of primary importance here. Their proof is omitted for brevity (see [Kuo, 1991]).

1. The $N = 0$ points on the root locus are at the poles of $C(s)P(s)$.

2. $N = \infty$ points on the root locus are at the zeroes of $C(s)P(s)$, including zeroes at infinity.

3. The root loci are symmetrical with respect to the real axis of the s-plane.

4. The root loci for $N > 0$ are found in a section of the real axis only if the total number of real poles and zeroes of $C(s)P(s)$ to the right of the section is odd.

For the class of systems of concern here one has

$$C(s)P(s) = \frac{K(K_D s^2 + K_C s + K_I)}{s(s+\lambda_1)(s+\lambda_2)}. \tag{3.13}$$

Assuming $K_D \neq 0$

$$C(s)P(s) = \frac{KK_D(s^2 + \frac{K_C}{K_D}s + \frac{K_I}{K_D})}{s(s+\lambda_1)(s+\lambda_2)} \tag{3.14}$$

$$= \frac{N(s+z_1)(s+z_2)}{s(s+\lambda_1)(s+\lambda_2)} \tag{3.15}$$

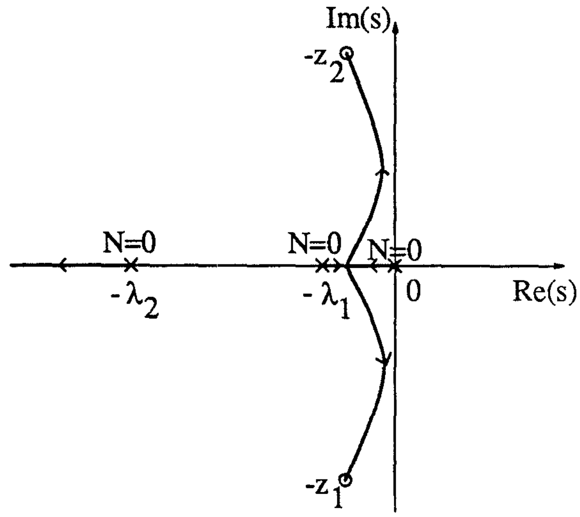

Figure 3.4: Root Locus of Class of Interest

where $N = KK_D$, and z_1 and z_2 are the controller zeroes. If N is varied keeping $\frac{K_C}{K_D}$ and $\frac{K_L}{K_D}$ constant a root locus of such a system is as given in Figure 3.4. This excludes the limiting case when $K_D = 0$, as then only one zero remains.

Since the system may have higher order poles, it is worthwile examining their influence on the general root locus characteristics. The root loci for two cases when there is 1) a pole $-\lambda_3$ with $\lambda_3 > \lambda_2$, and 2) a pair of complex conjugate poles with their real part equal to $-\lambda_2$ are illustrated in Figure 3.5. In both cases the real part of the root loci originating from the two poles of greater absolute magnitude is smaller than $-\lambda_2$. Hence, the dynamics due to the higher order poles are very fast, and are damped out quickly. Also note that the shape of the root locus due to the poles near the origin has remained more or less the same.

Hence, one can restrict ones attention to a second order open loop system

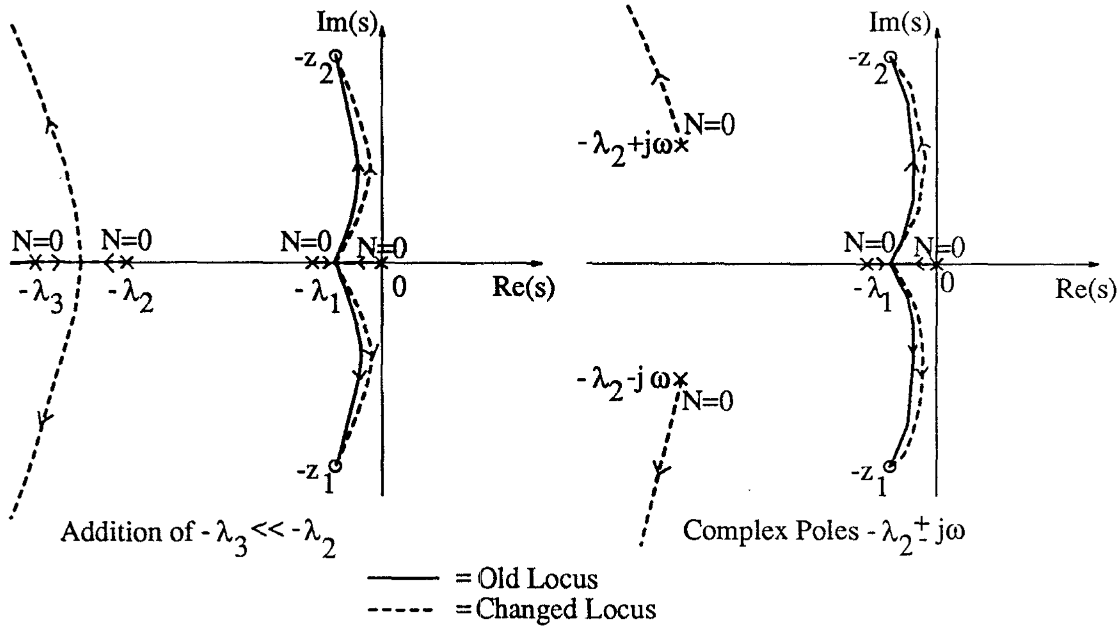

Figure 3.5: Effect of Additional Poles on the Root Locus

and concentrate on the behaviour of the root locus due to the pole closest to the origin. Thus, it is observed that the portion of the root locus of importance is not greatly influenced by the presence of unaccounted higher order poles.

3.5 Pole-Zero Placement

The portion of the root locus of interest is the one closest to the imaginary axis of the s-plane. Two of the roots of the characteristic equation

$$1 + C(s)P(s) = 0 \tag{3.16}$$

lie somewhere on this root locus, whereas the third root is further away from the origin, and hence its effect is quickly damped out. Hence the two dominant poles of the closed loop system lie on the root locus between the poles 0 and $-\lambda_1$ and

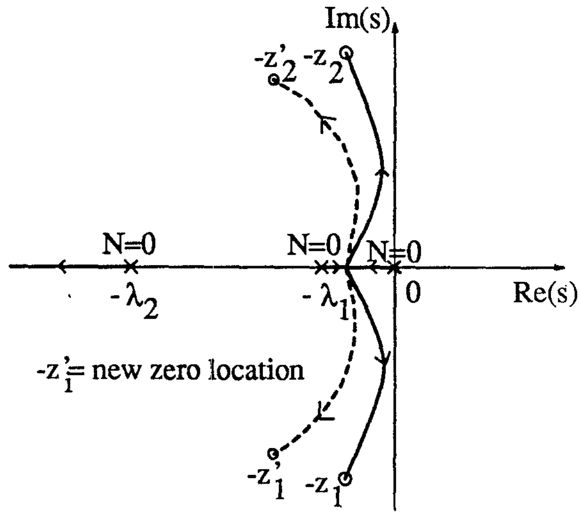

Figure 3.6: Effect of Movement of Zeroes on the Root Locus

the two zeroes of the controller z_1 and z_2.

The aim here is to determine the movement of these two poles due to movement of the controller zeroes. The latter are given by

$$z_1 = -\frac{K_C}{2K_D}\left(1 + \sqrt{1 - \frac{4K_D K_I}{K_C^2}}\right) \tag{3.17}$$

$$z_2 = -\frac{K_C}{2K_D}\left(1 - \sqrt{1 - \frac{4K_D K_I}{K_C^2}}\right) \tag{3.18}$$

and hence can be moved about by varying the PID gains K_C, K_D and K_I in a suitable manner.

It is intuitive to see that the non-real part of the root locus is *dragged* about by the movement of the zeroes of $C(s)$. This is illustrated in Figure 3.6. Hence, if the zeroes are moved away from the imaginary axis so is the root loci.

The movement of the poles as a result of the movement of zeroes can be seen more clearly by considering a simpler closed loop system (Appendix A gives a discussion on the effect of PID zeroes on the closed loop poles for the case of a second order plant). Let the system be given by

$$C(s)P(s) = \frac{K(s+z_1)(s+z_2)}{s(s+\lambda)} \tag{3.19}$$

where z_1 and z_2 are complex conjugate controller zeroes. The characteristic equation to be satisfied by the closed loop poles is given by

$$1 + C(s)P(s) = 1 + \frac{K(s+z_1)(s+z_2)}{s(s+\lambda)} = 0 \tag{3.20}$$

$\Rightarrow$

$$(1+K)s^2 + (\lambda + K(z_1+z_2))s + Kz_1z_2 = 0 \tag{3.21}$$

Assuming this to have complex conjugate roots p_1 and p_2 one obtains

$$p_1, p_2 = \nu \pm j\mu = -\frac{\lambda + K(z_1+z_2)}{2(1+K)} \pm j\frac{\sqrt{4Kz_1z_2(1+K) - (\lambda + K(z_1+z_2))^2}}{2(1+K)} \tag{3.22}$$

Letting z_1,$z_2 = \alpha \pm j\beta$ equation 3.22 can be written after seperating ν and μ as

$$\nu = -\frac{\lambda + 2\alpha K}{2(1+K)} \tag{3.23}$$

and

$$\mu = \frac{\sqrt{4K(\alpha^2+\beta^2)(1+K) - (\lambda + 2K\alpha)^2}}{2(1+K)} \tag{3.24}$$

$\Rightarrow$

$$\frac{d\nu}{d\alpha} = -\frac{K}{1+K} \tag{3.25}$$

$$\frac{d\mu}{d\alpha} = \frac{K(2\alpha - \lambda)}{(1+K)\sqrt{4K(\alpha^2+\beta^2)(1+K) - (\lambda + 2K\alpha)^2}} \tag{3.26}$$

$$\frac{d\nu}{d\beta} = 0 \tag{3.27}$$

$$\frac{d\mu}{d\beta} = \frac{2K\beta}{\sqrt{4K(\alpha^2 + \beta^2)(1 + K) - (\lambda + 2K\alpha)^2}} \tag{3.28}$$

It can be seen from equations 3.25-3.28 that the closed loop poles are influenced by the movement of the controller zeroes. If the zeroes are moved towards the imaginary axis, ν increases and the poles also move towards the imaginary axis. The movement of the imaginary part of the poles μ is not so straightforward as, the sign of $\frac{d\mu}{d\alpha}$ depends on the magnitude of α and λ. On the other hand the imaginary component of the controller zeroes influences only the imaginary part of the closed loop poles. It should be noted here that if $\alpha < \frac{\lambda}{2}$ then $\frac{d\mu}{d\alpha} < 0$ and hence, there is a region near the imaginary axis where $\frac{d\mu}{d\alpha} < 0$ as desired. Also note that

$$\frac{\mid \frac{d\mu}{d\beta} \mid}{\mid \frac{d\mu}{d\alpha} \mid} = \frac{2\beta(1 + K)}{\mid 2\alpha - \lambda \mid}. \tag{3.29}$$

Once $\alpha > \frac{\lambda}{2}$, the direction of change in the imaginary component of the poles is determined by this ratio. The larger this ratio, the more the influence of a change in β on the imaginary component of the poles(μ). In practice the change in β is made much larger than that for α for frame 1, so that it can influence the closed-loop poles to a still larger extent.

From the analysis of the class of interest presented in Appendix A, it is seen

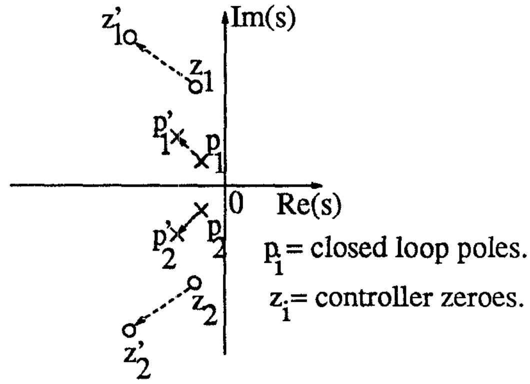

Figure 3.7: Effect of Moving Controller Zeroes on the Closed Loop Poles

that even this class of systems has a similar relationship between the controller zeroes and the closed-loop poles. Also, there exists a region near the imaginary axis, where $\frac{d\mu}{d\alpha} < 0$. Since chemical processes normally have a very large rise time, from equation 3.4, one gets $\omega \ll 1$. If this is true, then one obtains a reasonably large region where $\frac{d\mu}{d\alpha} < 0$. It seems that this region is sufficiently large for the purpose here, and this fact is further strengthened by simulation studies and the results presented in Chapter 5. Hence a significant control can be exerted on the poles of the closed loop system by moving the controller zeroes. This is shown in Figure 3.7.

On the premise, that the main purpose of the expert is to decrease the rise time, the actions for frame 1 are geared towards achieving this goal. If the poles are currently out of the region where $\frac{d\mu}{d\alpha} < 0$ and the response is faster than desired, then the poles are moved towards the imaginary axis in frame 2. This will be further elaborated upon below.

Based on all the above observations the following rules are postulated for influencing the damping factor and the natural frequency.

1. Frame 1

   (a) To decrease the damping factor and to increase the natural frequency, increase $\text{Re}(z_i)$ and increase $\text{Im}(z_i)$ by a greater amount.

   (b) To increase the damping factor and to decrease the natural frequency, decrease $\text{Re}(z_i)$ and decrease $\text{Im}(z_i)$ by a greater amount.

2. Frame 2

   (a) If the amplitude of oscillations is not *small* or the rate of change of error is not *zero* , then decrease $\text{Re}(z_i)$. As seen by the analysis presented above, if the zeroes are sufficiently close to the imaginary axis, the poles will move closer together and will cause the damping factor to increase. If however, the zeroes are further away then the natural frequency increases. Either way the settling time decreases.

   (b) Once the amplitude of oscillations is *small* , and the rate of change of error is *zero* , increase $\text{Re}(z_i)$ and increase $\text{Im}(z_i)$. This leads to a decrease in the damping factor, and aids in returning the response to steady state. This action is usually taken over a fixed period of time to prevent unwanted action due to measurement noise. This time is usually 4 to 5 times the response time (T_2) of the reference response.

Hence, if one wants to slow down a fast response due to poles which lie outside the region where $\frac{d\mu}{d\alpha} < 0$, then 2(b) above causes the controller zeroes and hence, the closed-loop poles to move towards the region of interest near the imaginary axis. This is because, with such an initial response the expert's actions are predominantly those in 2(b), as the amount of time spent by the system in frame 1 and in frame 2 with the response oscillation amplitude greater than *small* is very small compared to the fixed amount of time spent in the phase where actions in 2(b) are carried out. Thus the poles ultimately end up in the region of interest, and the expert can then compensate.

3.6 Discussion on Stability

If K_D, K_C and K_I are restricted to be positive, the controller zeroes are restricted to the left half of the s-plane. Hence if the closed loop system becomes unstable, it does through complex conjugate poles. This is illustrated Figure 3.8. Thus the only unstable response possible is an exponentially growing sinusoidal. This implies that the response enters frame 2, and once there the zeroes are moved away from the imaginary axis due to increased damping. Hence ultimately the root locus will be pulled back into the left half plane and the system stabilized.

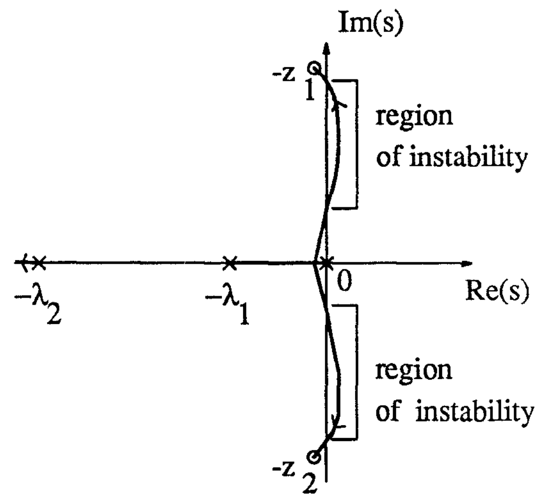

Figure 3.8: Root Locus Exhibiting Instability Due to Complex Conjugate Poles

3.7 Effect of Small Dead Time

The dead time is taken as a parameter in the specified response. Since that value is approximate, there may still be a small dead time present. This can be approximated by a second order Padè approximation as

$$e^{-t_D s} \approx \frac{t_D^2 s^2 - 6t_D s + 12}{t_D^2 s^2 + 6t_D s + 12} \qquad (3.30)$$

This gives rise to complex conjugate zeroes in the right half plane, and complex conjugate poles in the left half plane, all placed symmetrically around the origin. A root locus for such a system is shown in Figure 3.9.

By looking at the root locus, one can see that the system may become unstable. However, by decreasing the loop gain N, one can stabilize the system. This strategy works even for large dead times.

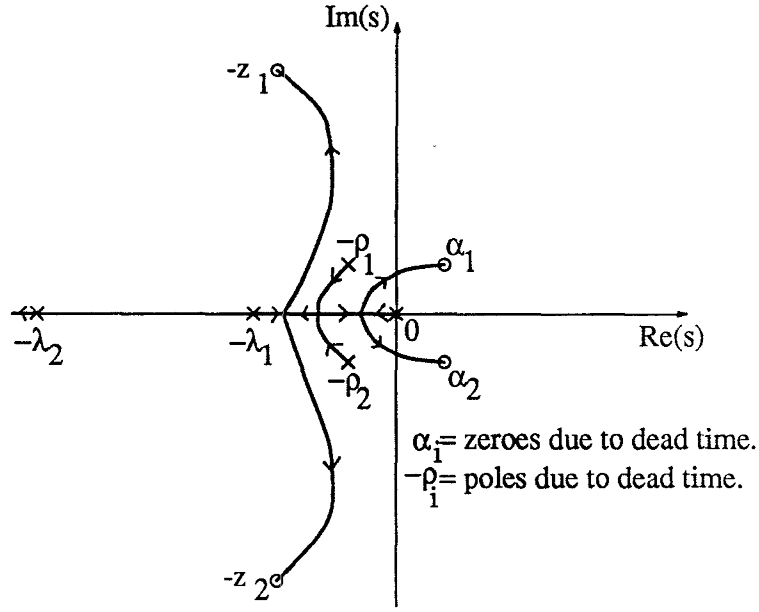

Figure 3.9: Effect of Small Dead Time on the Root Locus

3.8 Variation of Gain(N)

So far, the discussion has been concerned with the relationship between movement of controller zeroes and the movement of the closed-loop poles. However, one has to also consider the variation in the gain(N). Recalling equation 3.14, one has

$$N = KK_D \tag{3.31}$$

where K is the open-loop plant gain, and K_D is the derivative mode gain. For the moment assume that the controller zeroes are fixed. Varying N results in the movement of the closed-loop poles along the root locus. The larger the value of N, the closer the closed-loop poles are to the controller zeroes. The net movement of the closed-loop poles is the combination of, the movement due to the movement in the controller zeroes and the movement due to a change in N. Hence for varying

N, the following rules are postulated.

1. Frame 1

   (a) If the response is very slow then, increase N. This results in an increase in the natural frequency(ω).

   (b) If the response is very fast then, decrease N. This results in a decrease in the natural frequency.

   The effect on the damping factor(ξ) depends on the shape of the root locus (which in turn depends on the location of the controller zeroes). However, as seen by equation 3.4, the effect of ξ on the rise time is much smaller than the effect of ω.

2. Frame 2

   (a) Initially, if the amplitude of oscillations is not *small* or the rate of change of error is not *zero* , then decrease N. This will result in an increase in ξ. This tends to help damp out oscillations.

   (b) If the amplitude of oscillations is *small* and the rate of change of error is *zero* then the gain N is increased. The chief aim of doing so is to move the complex closed-loop poles back towards the controller zeroes. This increases ω, and helps speed up the return of the response to the steady state value.

$e_1(t)$	Δ_{K_C}	Δ_{K_D}	Δ_{K_I}
PL	NL	PS	PL
PM	NM	Z	PM
PS	NS	Z	PS
Z	Z	Z	Z
NS	PS	Z	NS
NM	PM	Z	NM
NL	PL	NS	NL

Table 3.1: Rules for Frame 1

3.9 PID Gain Variation

After all the discussion, the rules to vary K_C, K_D and K_I are now presented. Since K_D is the only parameter which influences the gain N, its variation is determined by the manner in which N has to be changed as discussed in Section 3.8. It should be noted that

$$\Delta N \approx K \Delta K_D. \tag{3.32}$$

K_C and K_I are varied to ensure that in conjunction with the variation in K_D as obtained above, the controller zeroes move as discussed in Section 3.7. The issue is further complicated by the dependence of the changes in $\mathrm{Re}(z_i)$ and $\mathrm{Im}(z_i)$ on the values of the PID gains. Appendix B gives an approximate analysis of the effect of varying the PID gains on the controller zeroes. The actual rules used to implement the PID gain variations are illustrated in Table 3.1 for frame 1, and in Table 3.2 for frame 2.

Though the analysis in the Appendix B illustrates that these rules work for

$e_2(t)$	$\frac{de_2(t)}{dt}$ PL	PM	PS	Z	NS	NM	NL
PL	Z	Z	Z	Z	PS	PS	PM
PM	Z	Z	Z	Z	PS	PM	PM
PS	Z	Z	Z	NS	PS	PM	PM
Z	Z	Z	Z	Z	Z	Z	Z
NS	PM	PM	PS	NS	Z	Z	Z
NM	PM	PM	PS	Z	Z	Z	Z
NL	PM	PS	PS	Z	Z	Z	Z

Δ_{K_C}

$e_2(t)$	$\frac{de_2(t)}{dt}$ PL	PM	PS	Z	NS	NM	NL
PL	Z	Z	Z	Z	NM	NM	NL
PM	Z	Z	Z	Z	NM	NL	NL
PS	Z	Z	Z	PS	NM	NL	NL
Z	Z	Z	Z	Z	Z	Z	Z
NS	NL	NL	NM	PS	Z	Z	Z
NM	NL	NL	NM	Z	Z	Z	Z
NL	NL	NM	NM	Z	Z	Z	Z

Δ_{K_D}

$e_2(t)$	$\frac{de_2(t)}{dt}$ PL	PM	PS	Z	NS	NM	NL
PL	Z	Z	Z	Z	NS	NS	NM
PM	Z	Z	Z	Z	NS	NM	NM
PS	Z	Z	Z	PS	NS	NM	NM
Z	Z	Z	Z	Z	Z	Z	Z
NS	NM	NM	NS	PS	Z	Z	Z
NM	NM	NM	NS	Z	Z	Z	Z
NL	NM	NS	NS	Z	Z	Z	Z

Δ_{K_I}

Table 3.2: Rules for Frame 2

particular ranges of the gains, the general case seems to be unclear. However simulation results have proven encouraging.

Chapter 4

Implementation Issues

This chapter discusses some of the issues concerned with constructing the expert. The fuzzy membership functions for the measured quantities and the outputs are defined. The idea of scaling the outputs to obtain the actual PID gain variation is discussed. A brief note on the duration of the expert's action is made.

4.1 Fuzzy Membership Functions

This section discusses the fuzzy membership functions for $e_1(t)$, $e_2(t)$, $\frac{de_2(t)}{dt}$, and the output set (Δ). The output set is the same for all three of the PID parameters K_C, K_D and K_I. Scaling is used to obtain their actual numerical values (ΔK_C, ΔK_D and ΔK_I), from the unscaled values δ_{K_C}, δ_{K_D} and δ_{K_I}.

These membership functions are best represented as figures. Figure 4.1 shows the membership functions. Note that for the error membership functions, there is a region around zero, that belongs only to the *Zero* membership function. This is for the purposes of noise immunity. Since all the values are assumed to range from -1 to +1, the measured values need to be scaled, before their membership can be evaluated.

i.e. $e_1\prime(t) = \eta_1 e_1(t)$, $e_2\prime(t) = \eta_2 e_2(t)$, and $\frac{de\prime_2(t)}{dt} = \eta_3 \frac{de_2(t)}{dt}$. These $\prime$ values are then used to evaluate the membership values of the respective inputs.

Membership functions, though can be of any shape have been chosen here to be triangular. This is to reduce the computational complexity in evaluating the membership values. Once these are evaluated, the classification(s) (NL,NS etc.) and their membership values are passed onto the rule evaluator.

4.2 Rule Evaluation and Scaling of Outputs

There are two sets of rules used to determine the outputs.

1. One set is used during frame 1 to adjust the rise time.
2. The second set is used during frame 2 to damp out oscillations.

The rule evaluation block is told which frame the response is in and applies the corresponding set of rules. These rules are implemented as a set of if-then clauses as described in Section 2.2.

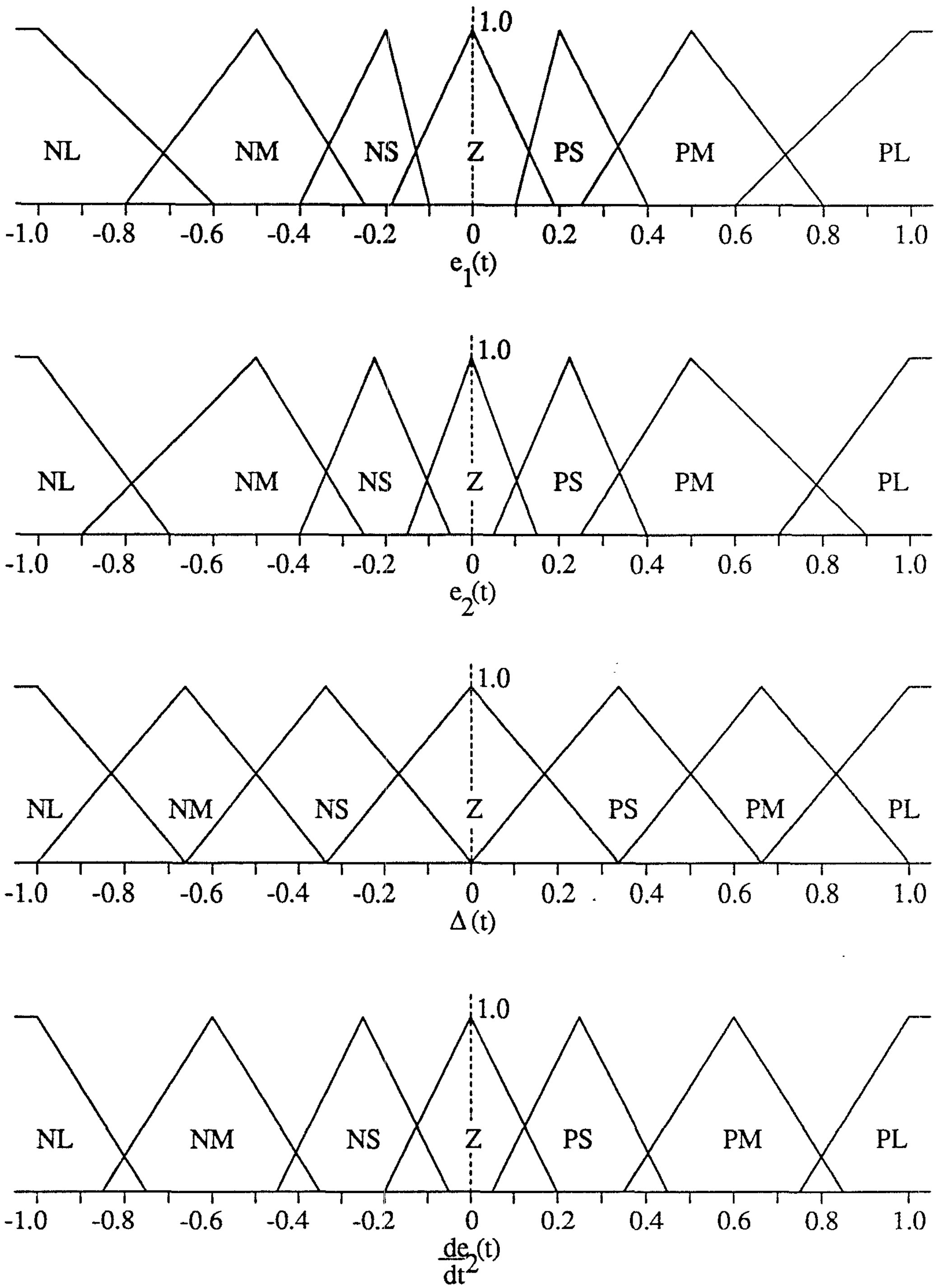

Figure 4.1: Fuzzy Membership Functions

After the rules are evaluated, the numerical values of Δ_{K_C}, Δ_{K_D} and Δ_{K_I} are evaluated by applying equation 2.6. Let these be represented by δ_{K_C}, δ_{K_D} and δ_{K_I}. From these the actual outputs are obtained after scaling as

$$\Delta K_C = \rho_{K_C}[K_{C_{max}} - K_{C_{min}}]\delta_{K_C} \tag{4.1}$$

$$\Delta K_D = \rho_{K_D}[K_{D_{max}} - K_{D_{min}}]\delta_{K_D} \tag{4.2}$$

$$\Delta K_I = \rho_{K_I}[K_{I_{max}} - K_{I_{min}}]\delta_{K_I} \tag{4.3}$$

where ρ_{K_C}, ρ_{K_D}, ρ_{K_I} represent sensitivities, $K_{C_{max}}$, $K_{D_{max}}$, $K_{I_{max}}$ the maximun allowed values of the gains, and $K_{C_{min}}$, $K_{D_{min}}$ and $K_{I_{min}}$ the minimun values of the gains.

In practice the expert will be operating in systems with measurement noise. Since the expert, as described so far has no means of knowing when the response is in steady state, it will mistake deviations due to noise as oscillations and hence will keep increasing the damping. To avoid this additional logic needs to be incorporated to inform the expert of the achievement of steady state. This is done by using a timer which starts once the amplitude of oscillation about the steady state value is within *small* . After a certain time, usually 4 to 5 times the response time T_2 the expert is deactivated. For all the results presented in the next chapter, this timer is incorporated in the expert.

The overall architecture of the expert is shown in Figure 4.2. FLC_1 and FLC_2 refer to two fuzzy logic controllers having an internal structure as shown

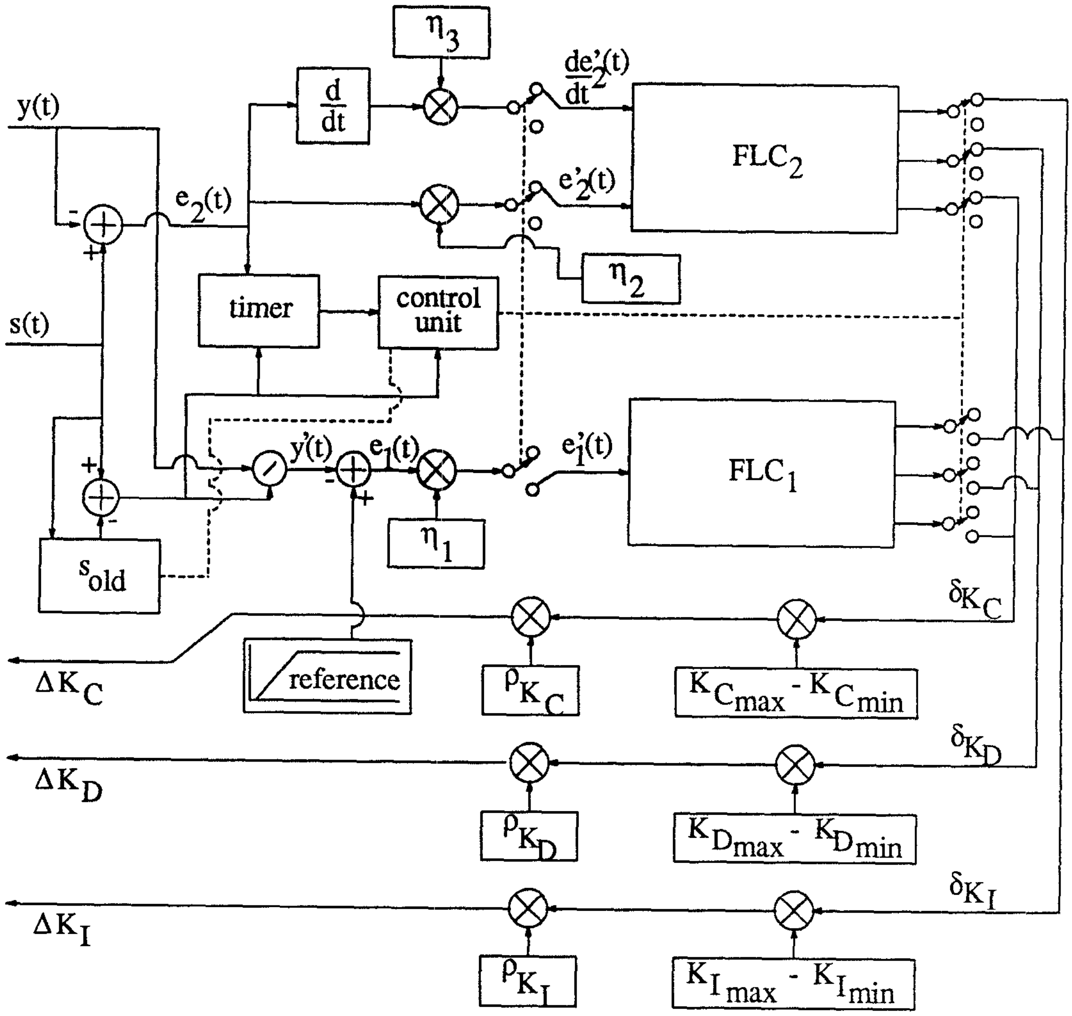

Figure 4.2: Architecture of the Expert (Shown Operating in Frame 2 Mode)

in Figure 2.3. The scaling factors η_1, η_2 and η_3 are chosen depending on the reference response desired. In the applications discussed, $\eta_1 = \eta_2 = 1$ was found to be sufficient. However η_2 should be chosen depending upon the expected overshoot, but its value is not critical in the sense that after the gains have stabilized. the response will be well behaved, and hence a not too large overshoot maybe expected. η_3 is chosen so that the slope of the reference response ($= \frac{1}{T_2}$) falls between *Medium* and *Large* .

The output sensitivities ρ_{K_C}, ρ_{K_D} and ρ_{K_I} are chosen depending on how much rate of change of the gains is allowable. If nothing is known about the process, conservative values can be chosen e.g. 0.001 used for the separator temperature control in the Tennessee Eastman Problem. The gain ranges are usually set by the PID controller limitations. They are incorporated so as to scale the *Positive/Negative Large* value of the output set to correspond to the full range of the controller gains. Since one would expect the actual gain values to be of the same order of magnitude as their respective ranges, these ranges also prove useful in the analysis presented in the Appendix B.

4.3 Overshoot Control and Adaptive Scaling

1. Overshoot Monitor:

   So far, the expert has no means of dealing with overshoot. Although, simulation studies show that usually the amount of overshoot is small, it may not be small enough. For this purpose an overshoot controller is built on top of the expert. It measures two quantities i) the maximum overshoot, and ii) the rise time. It should be noted here that priority is now given to control of the overshoot, rather than the control of rise time. This is in contrast to the original expert, which gave priority to the control of rise time. The overshoot controller tries to ensure that the overshoot is less than the prescribed maximum, while at the same time keeping the rise time as close to that of the reference response as possible.

To achieve this, the overshoot controller adaptively adjusts the switching point between frame 1 and frame 2. The action taken is proportional to the amount of overshoot, and is taken only if the overshoot exceeds the prescribed maximum. In particular, if the overshoot is larger than the maximum allowed, the expert is switched into the frame 2 mode sooner. If the overshoot requirement is satisfied, but the rise time requirement is not, then the expert is forced to remain in the frame 1 mode for a longer duration.

2. Adaptive Scaling:

The scaling factors (η_2 and η_3) for frame 2, are adaptively changed from iteration to iteration depending upon the maximum error ($e_{2_{max}}$), and the maximum rate of change of error ($(\frac{de_2}{dt})_{max}$) during the previous iteration. In particular, the rules are

$$if \ \mid e_{2_{max}} \mid > \ A_{noise} \ then \ \eta_2 = \frac{1.2}{\mid e_{2_{max}} \mid}$$

and

$$if \ \mid (\frac{de_2}{dt})_{max} \mid > \ B \ then \ \eta_3 = \frac{1}{\mid (\frac{de_2}{dt})_{max} \mid} \ .$$

where A_{noise} is the maximum noise amplitude and, B is a small number chosen to limit the magnitude of η_3. For example in the application presented in Section 5.4 $A_{noise} = 0.1$ and, $B = 0.001$ were chosen. This adaption of the scaling factors results in a more uniform action by the expert during frame

2. In fact it, enables the expert to damp out oscillations.

To evaluate the performance of the overshoot controller and adaptive scaling, an application is considered in Chapter 5 where the expert alone fails to give a satisfactory response in terms of the overshoot and oscillations about the steady state value.

Chapter 5

Applications

This chapter presents some applications of the expert described in the preceeding chapters. These are

1. To a known second order plant.
2. For the separator temperature control in the Tennessee Eastman Test Problem [Vogel and Downs, 1990].
3. To a third order plant.

The results of these applicatons are presented graphically in the following pages. The results for the third order plant are presented to verify the claim made in Section 3.4 concerning the robustness of the root locus with respect to addition of higher order poles. In the above applications, the expert is applied without the overshoot controller, and with fixed scale factors for frame 2. It is observed that the expert is unable to satisfactorily compensate the PID gains for the seperator temperature loop in the presence of liquid level change. More specifically, it results in a highly under damped response. This case is taken up again in Section 5.4, where the expert is applied along with the overshoot controller and with adaptive scaling.

5.1 Second Order Plant

The plant considered has the following transfer function

$$P(s) = \frac{Y(s)}{U(s)} = \frac{0.0301}{(s+0.003)(s+10)} \tag{5.1}$$

Here λ_1 = -0.003, λ_2 = -10 and $\lambda_2 \ll \lambda_1$.

The desired response has T_1 = 50 seconds and T_2 = 700 seconds. This is shown in Figure 5.1.

Two initial closed loop responses are considered

1. The initial PID parameters yield a very large rise time.

2. The closed loop system is initially unstable.

For both the cases the following parameters are selected for the expert.

$\eta_1 = \eta_2 = 1$, $\eta_3 = 60$, $\rho_{K_C} = \rho_{K_D} = \rho_{K_I} = 0.0005$, $K_{C_{max}} = 2$, $K_{C_{min}} = 0$, $K_{D_{max}} = 500$, $K_{D_{min}} = 0$, $K_{I_{max}} = 0.5$, and $K_{I_{min}} = 0.00001$.

A set-point change from 0 to 10 is considered in both cases.

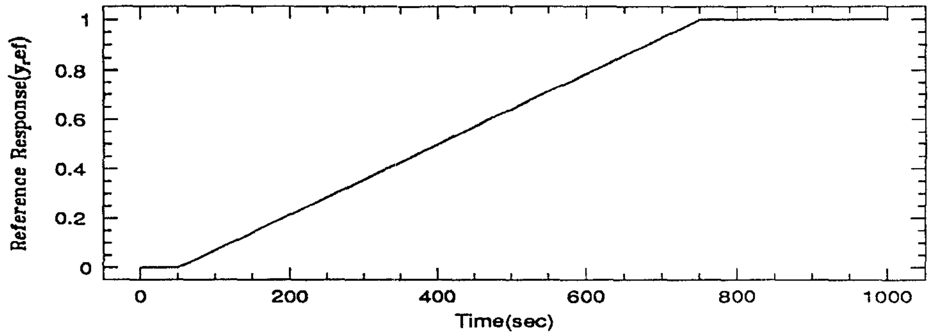

Figure 5.1: Second Order Plant: Reference Response

For the case with a large initial rise time, the initial response and the final response after the expert has tuned the gains is shown in Figure 5.2. Figure 5.3 shows the variation of the steady state gain values from iteration to iteration. The expert also acts as a gain scheduler, and the gain variation during a set-point change is shown in Figure 5.4.

Figure 5.5 illustrates the application of the expert to the case of an unstable initial response. The stabilizing feature of the expert can be seen by comparing the initial unstable response to the response during the first iteration. The final response is also illustrated. The gain variation from iteration to iteration is illustrated in Figure 5.6, and the gain scheduling behaviour is shown in Figure 5.7.

It is seen that in both the cases the expert greatly improves the closed loop response, moving it close to the desired response.

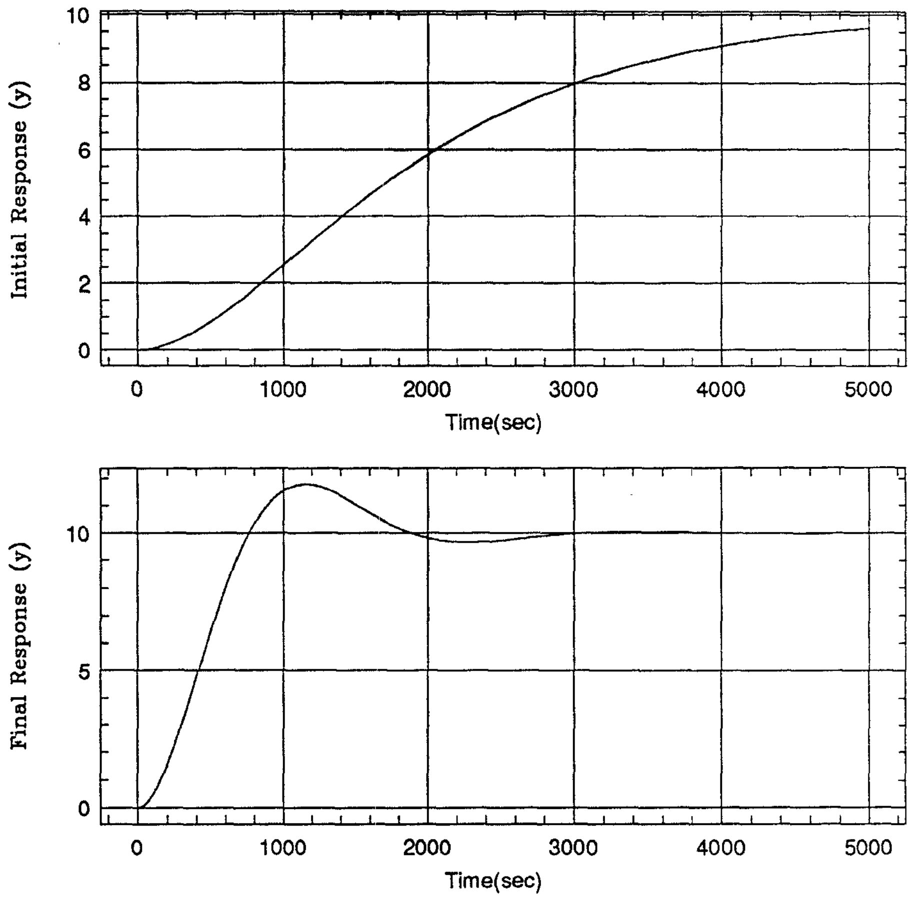

Figure 5.2: Second Order Plant: Very Slow Initial Response (top), Final Response (bottom)

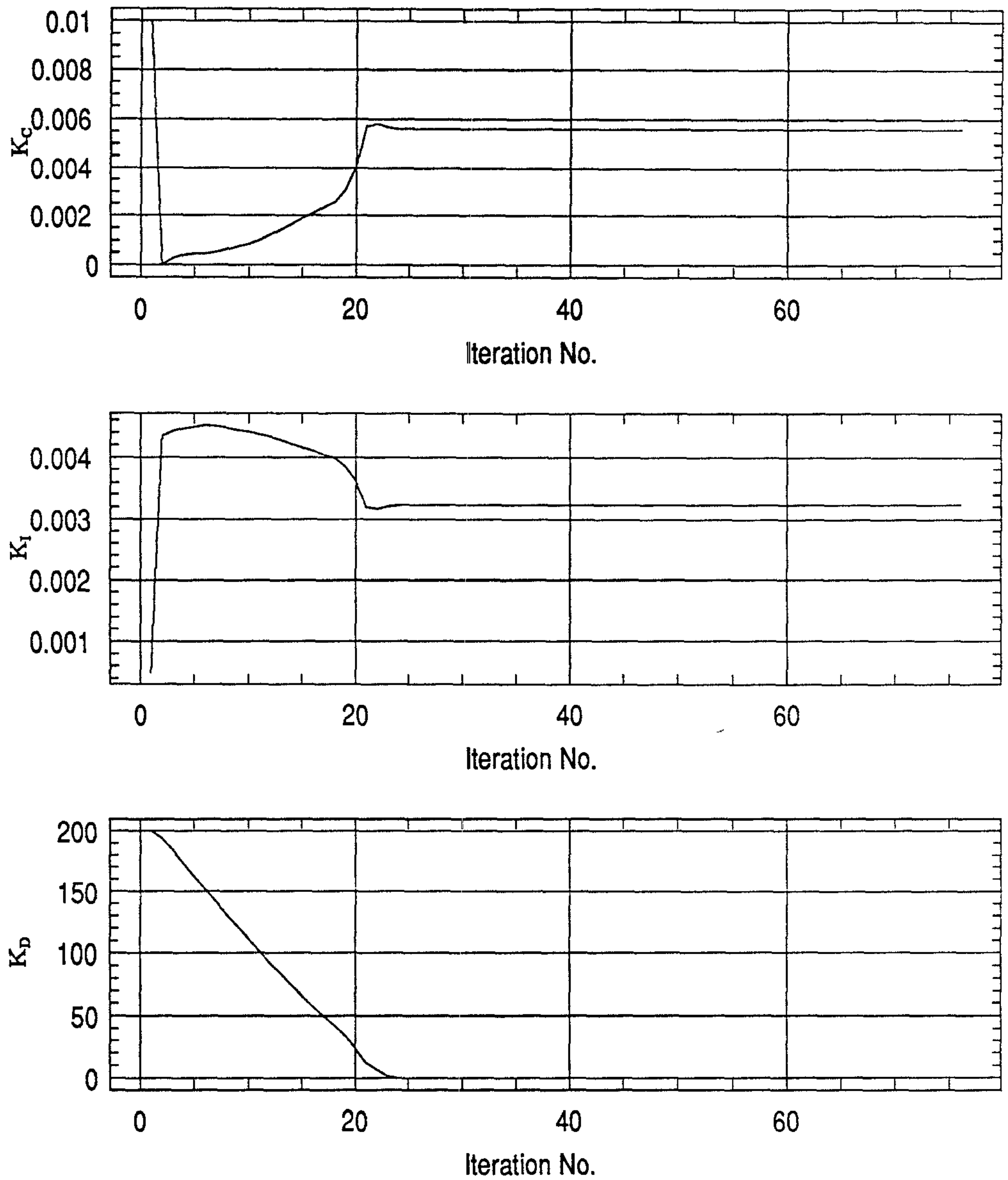

Figure 5.3: Second Order Plant(Initially Slow): Steady State Gains Versus Iteration Number

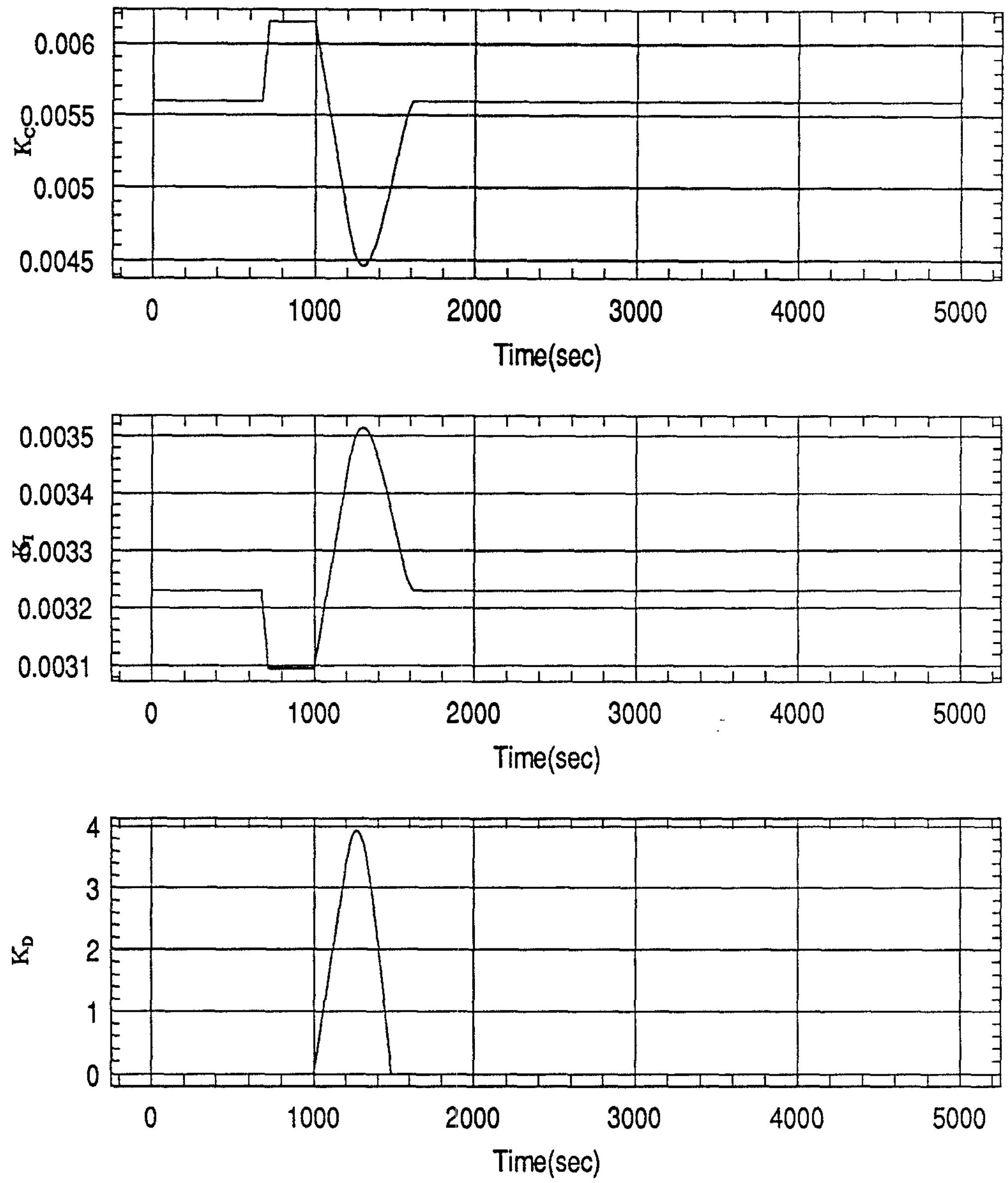

Figure 5.4: Second Order Plant(Initially Slow): Gain Scheduling During the Final Response

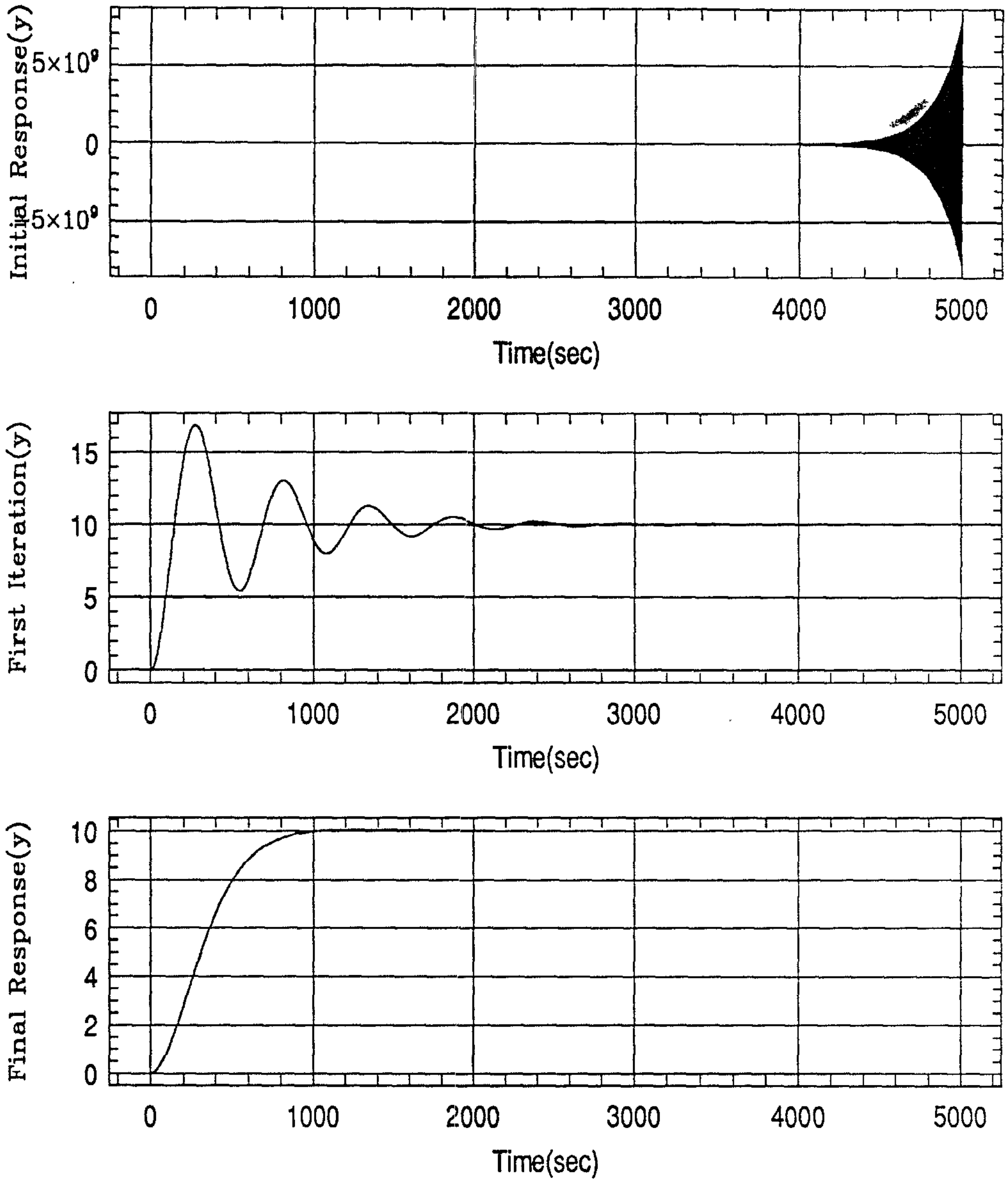

Figure 5.5: Second Order Plant: Unstable Initial Response(top), First Iteration Response(middle), Final Response(bottom)

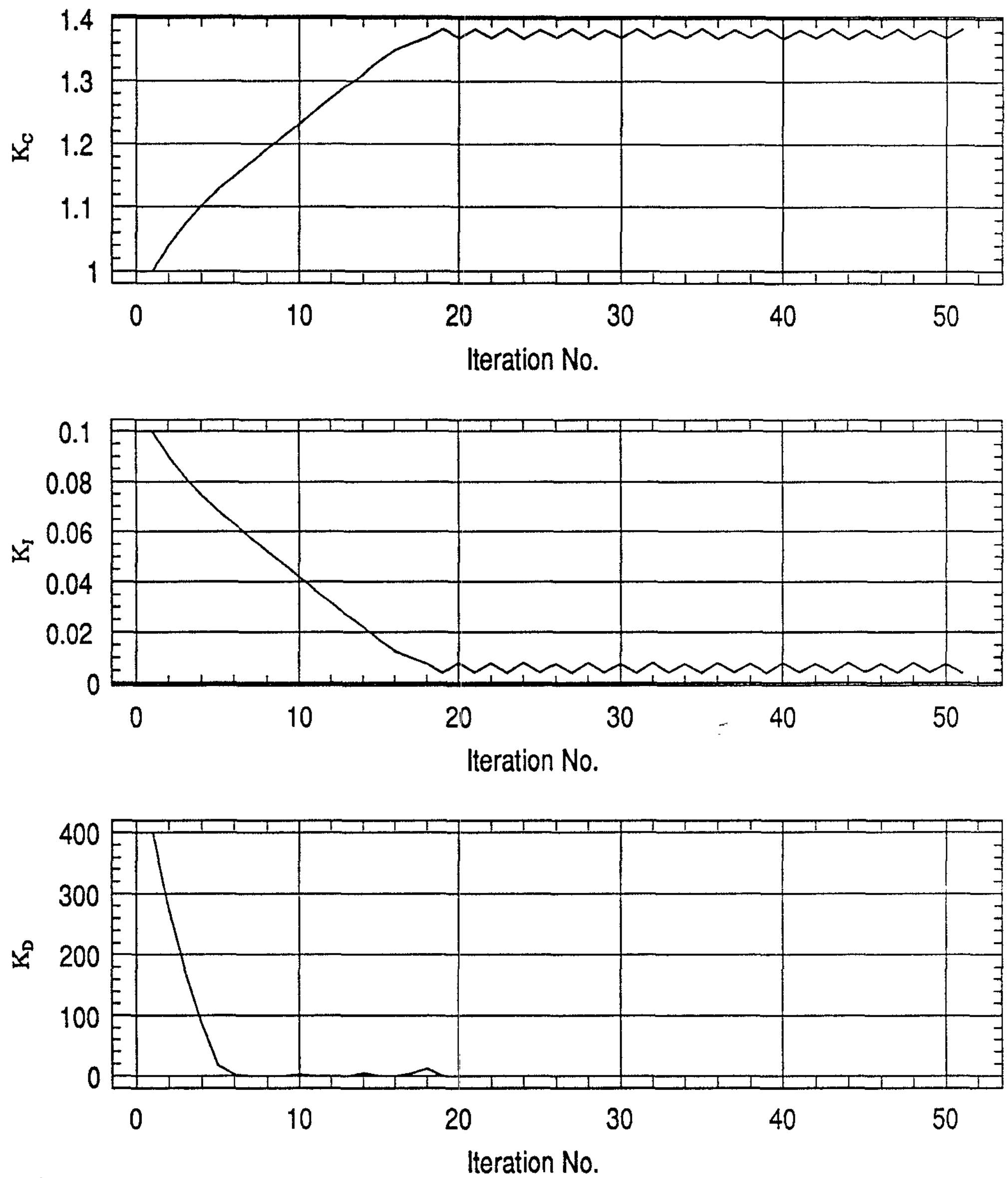

Figure 5.6: Second Order Plant(Initially Unstable): Steady State Gains Versus Iteration Number

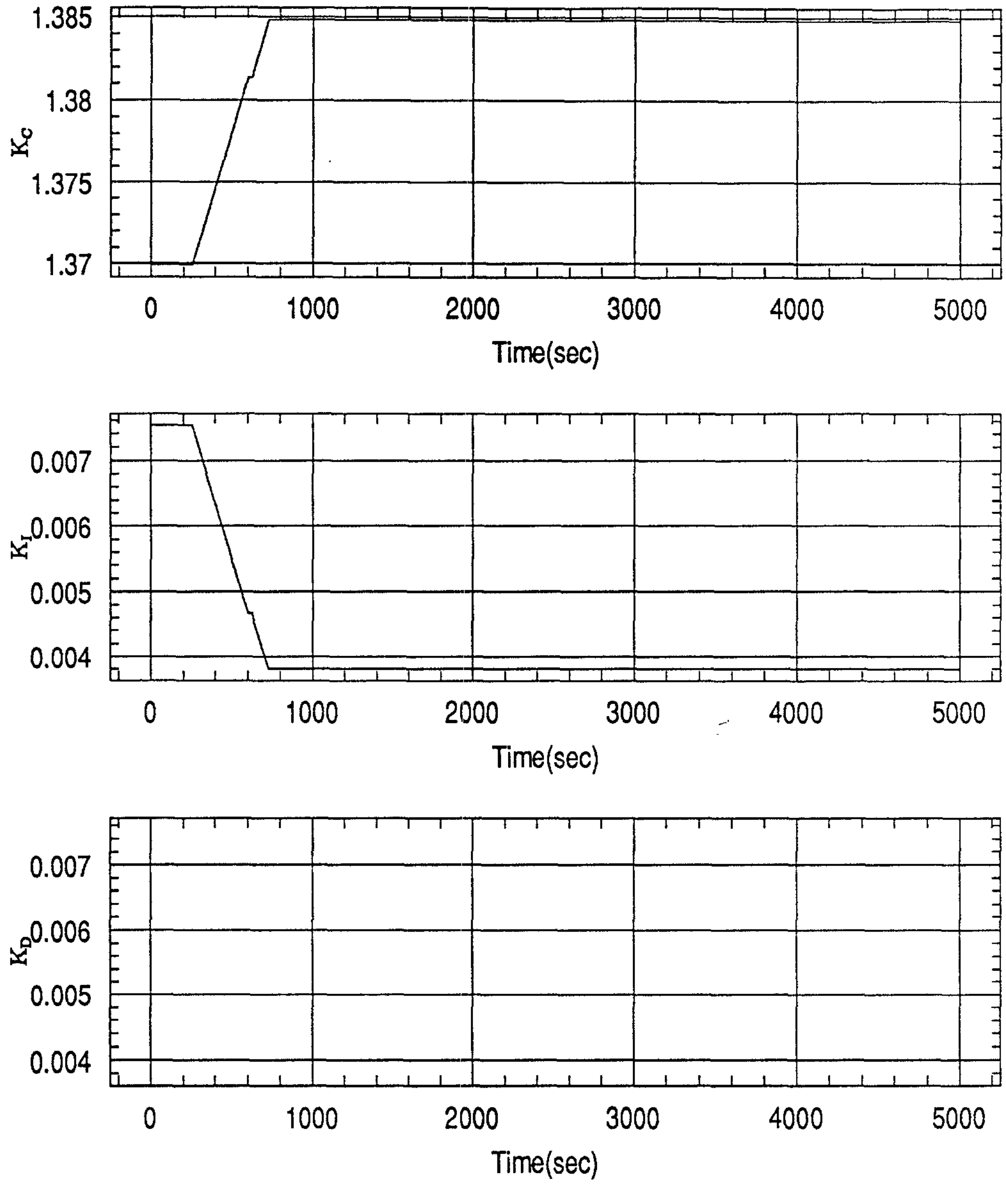

Figure 5.7: Second Order Plant(Initially Unstable): Gain Scheduling During the Final Response

5.2 Separator Temperature Control

The expert is applied to tune the PID parameters of the separator temperature control loop in the Tennessee Eastman Test Problem. Figure 5.8 shows the diagram of the process. For the purposes of separator temperature control, the condensor cooling water valve is chosen as the manipulated variable, and the separator temperature as the measured variable. The separator along with the chosen control loop is illustrated in Figure 5.9. This system has i)measurement noise, ii)an unknown number of plant poles, iii)measurement noise, and iv)bounds on the manipulated variables. Figure 5.10 shows the open loop response to a negative step change in the condensor cooling water flow. Two initial closed loop responses are considered here.

1. Initial PID settings give a very slow rise time.

2. The initial closed loop response is oscillatory.

Since the plant gain is negative, the input to the plant is multiplied by -1, to enable the use of positive controller gains. The adaptive property of the expert is also illustrated by changing the liquid level in the separator from 50% to 70%. Increasing the liquid level changes the plant characteristics and leads to a slower open loop response. The following parameters were used for the expert.

$\eta_1 = \eta_2 = 1$, $\eta_3 = 50$, $\rho_{K_C} = \rho_{K_D} = \rho_{K_I} = 0.001$, $K_{C_{max}} = 15$, $K_{C_{min}} = 2$,

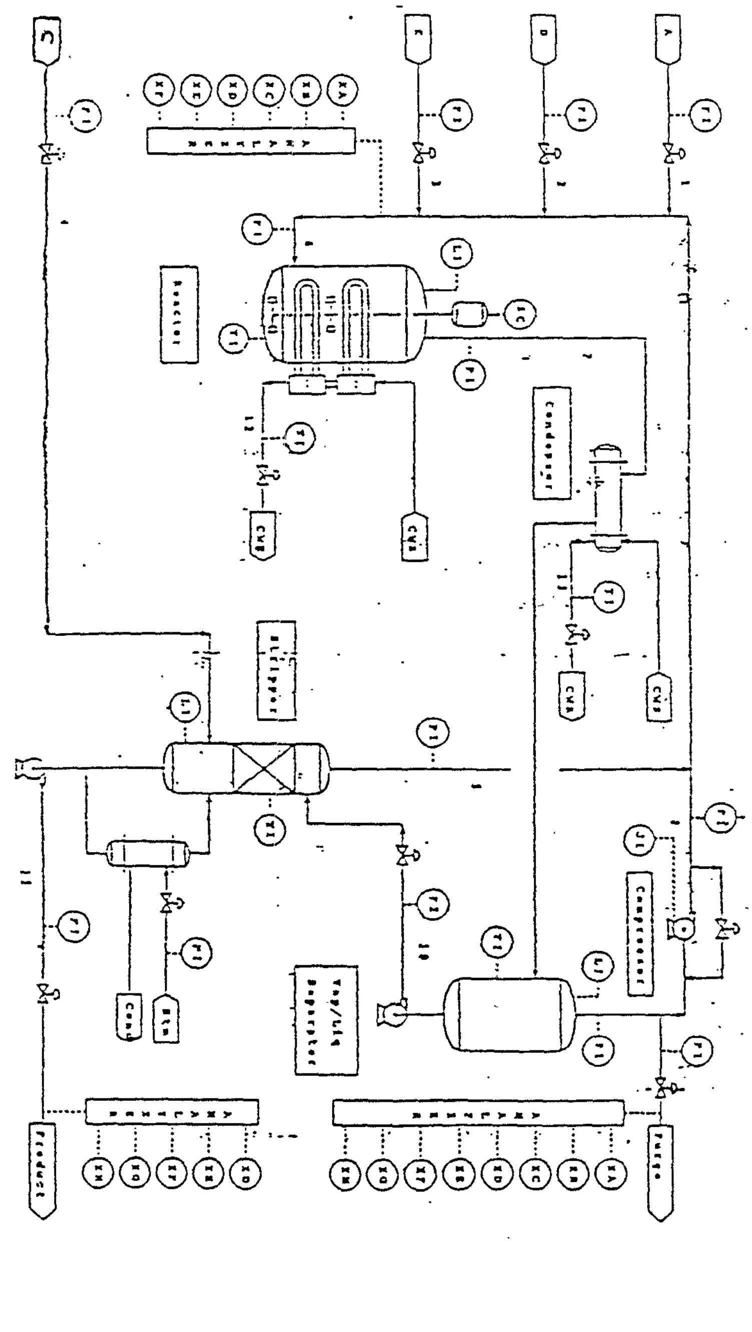

Figure 5.8: Tennessee Eastman Test Problem

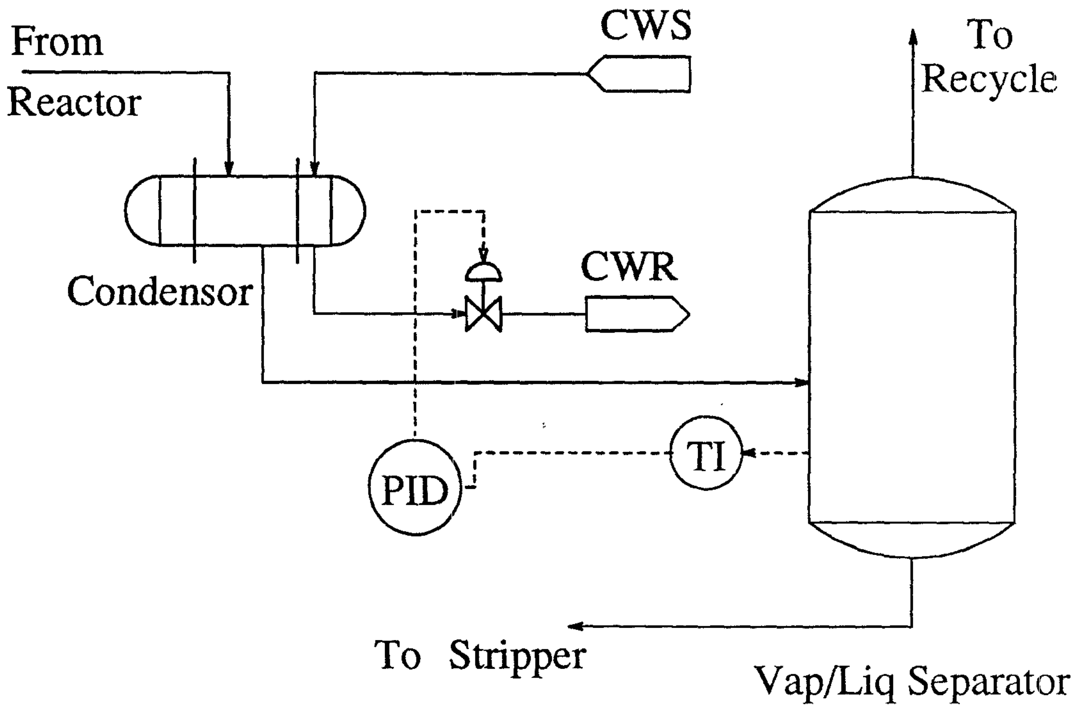

Figure 5.9: Separator: Chosen Control Loop

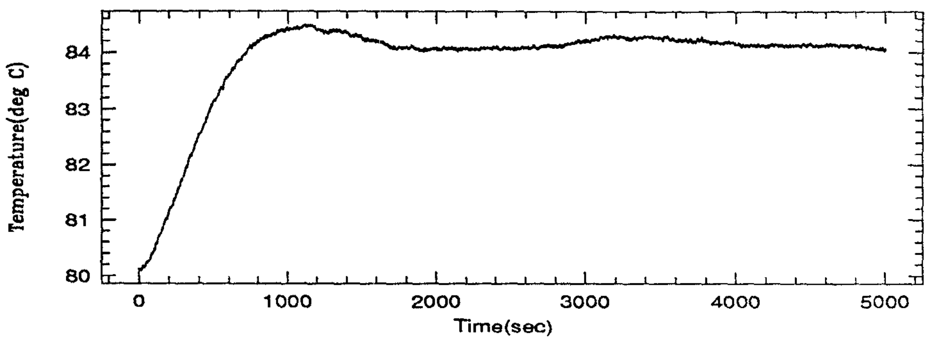

Figure 5.10: Separator: Open Loop Response

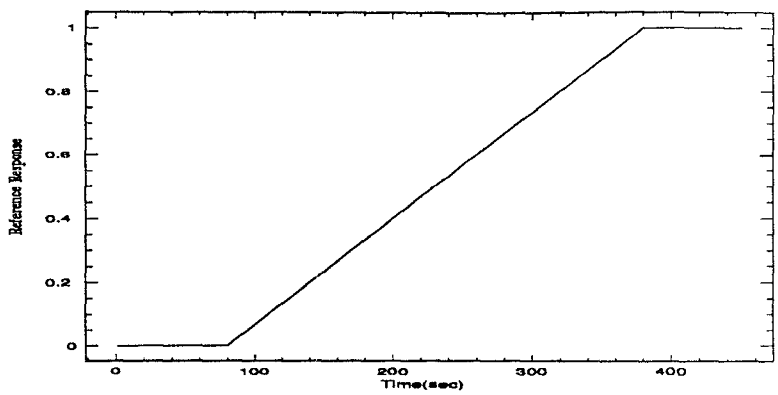

Figure 5.11: Separator: Reference Response

$K_{D_{max}} = 600$, $K_{D_{min}} = 0$, $K_{I_{max}} = 0.1$, and $K_{I_{min}} = 0.01$.

The reference response has $T_1 = 80$ seconds, and $T_2 = 300$ seconds. This is shown in Figure 5.11. A set-point change from 80.109 deg C to 85 deg C is chosen.

Figure 5.12 illustrates the initial and final responses for the large initial rise time case. The change in the steady state gain values from iteration to iteration is illustrated in Figure 5.13, and the gain scheduling behaviour can be observed in Figure 5.14.

Modification of the initially oscillatory closed loop behaviour is illustrated in Figure 5.15. It is seen that the oscillations are damped out in the first iteration itself. The final response is found to be close to the desired one. Changes in the steady state gains from iteration to iteration is shown in Figure 5.16, and the gain scheduling behaviour can be see in Figure 5.17.

Once the response is close to the desired one, the liquid level in the separator is changed from 50% to 70%. This changes the characteristics of the system. This

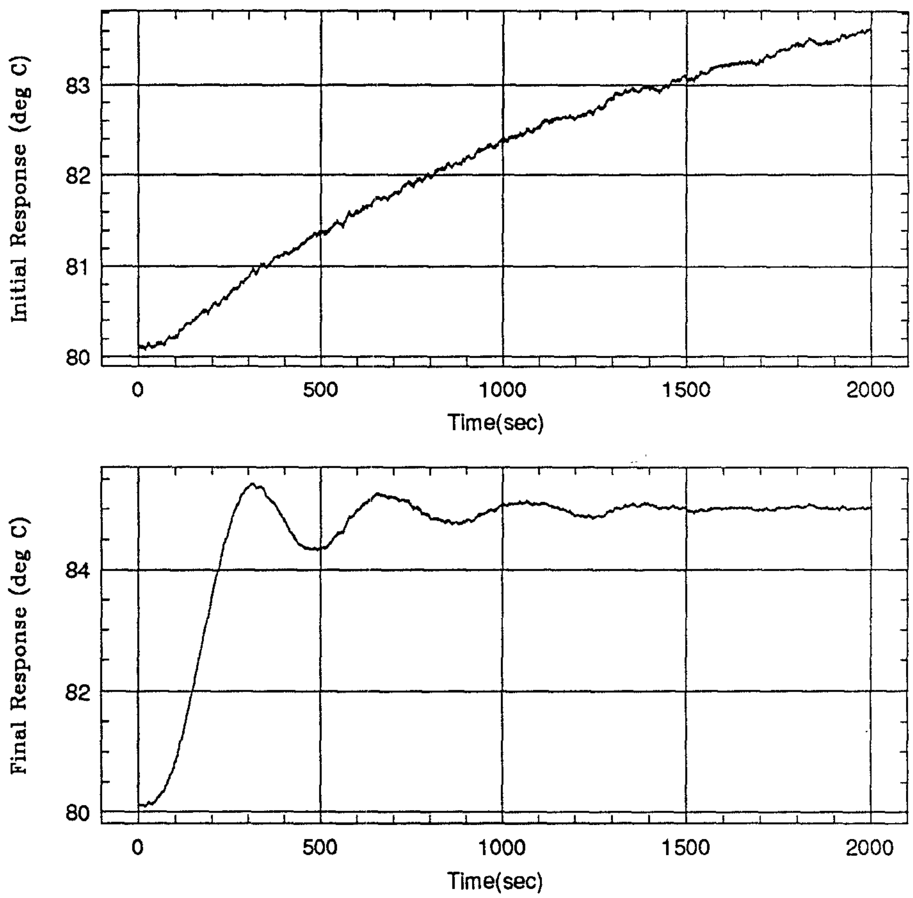

Figure 5.12: Separator: Very Slow Initial Response(top), Final Response(bottom)

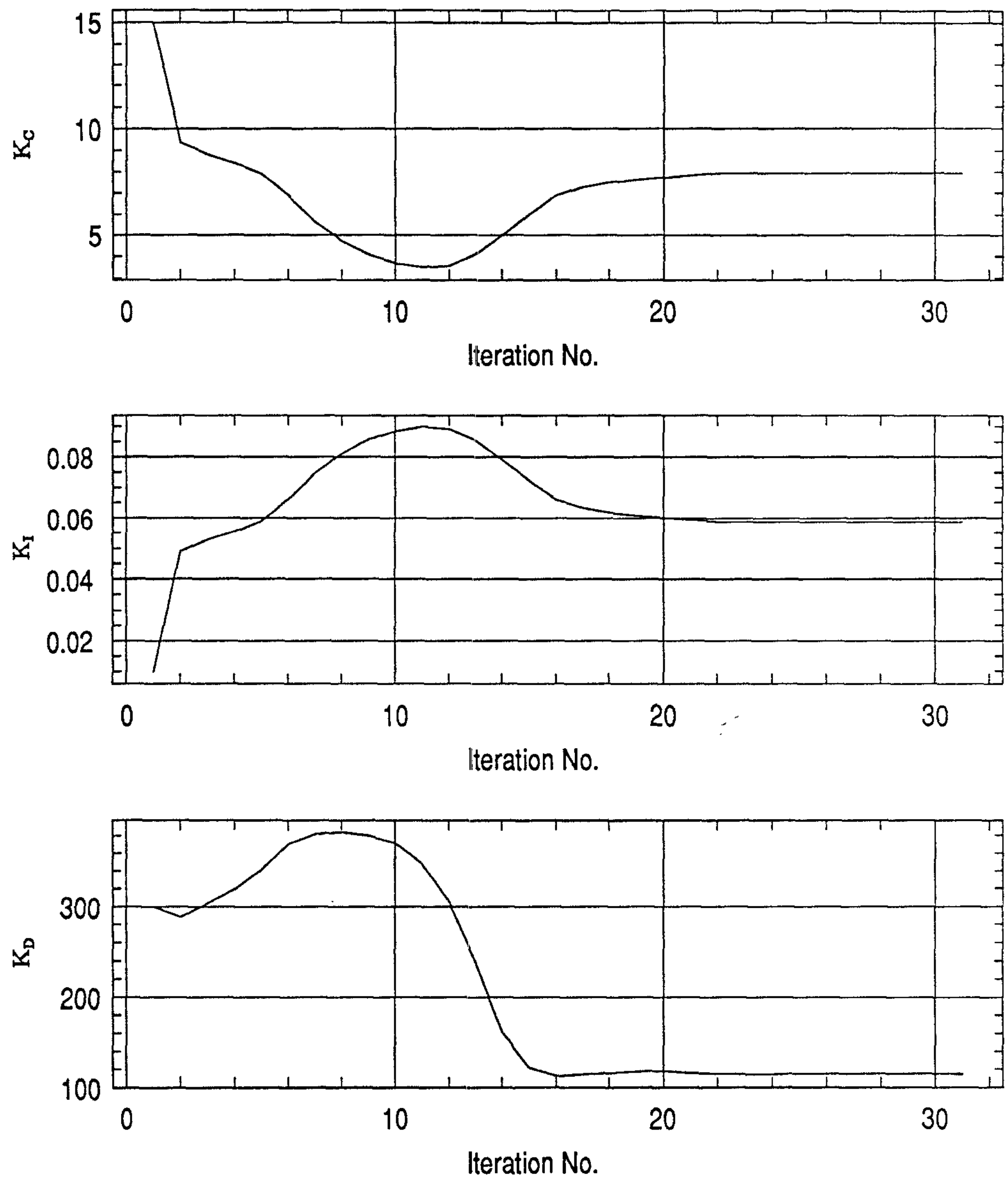

Figure 5.13: Separator(Initially Slow): Steady State Gains Versus Iteration Number

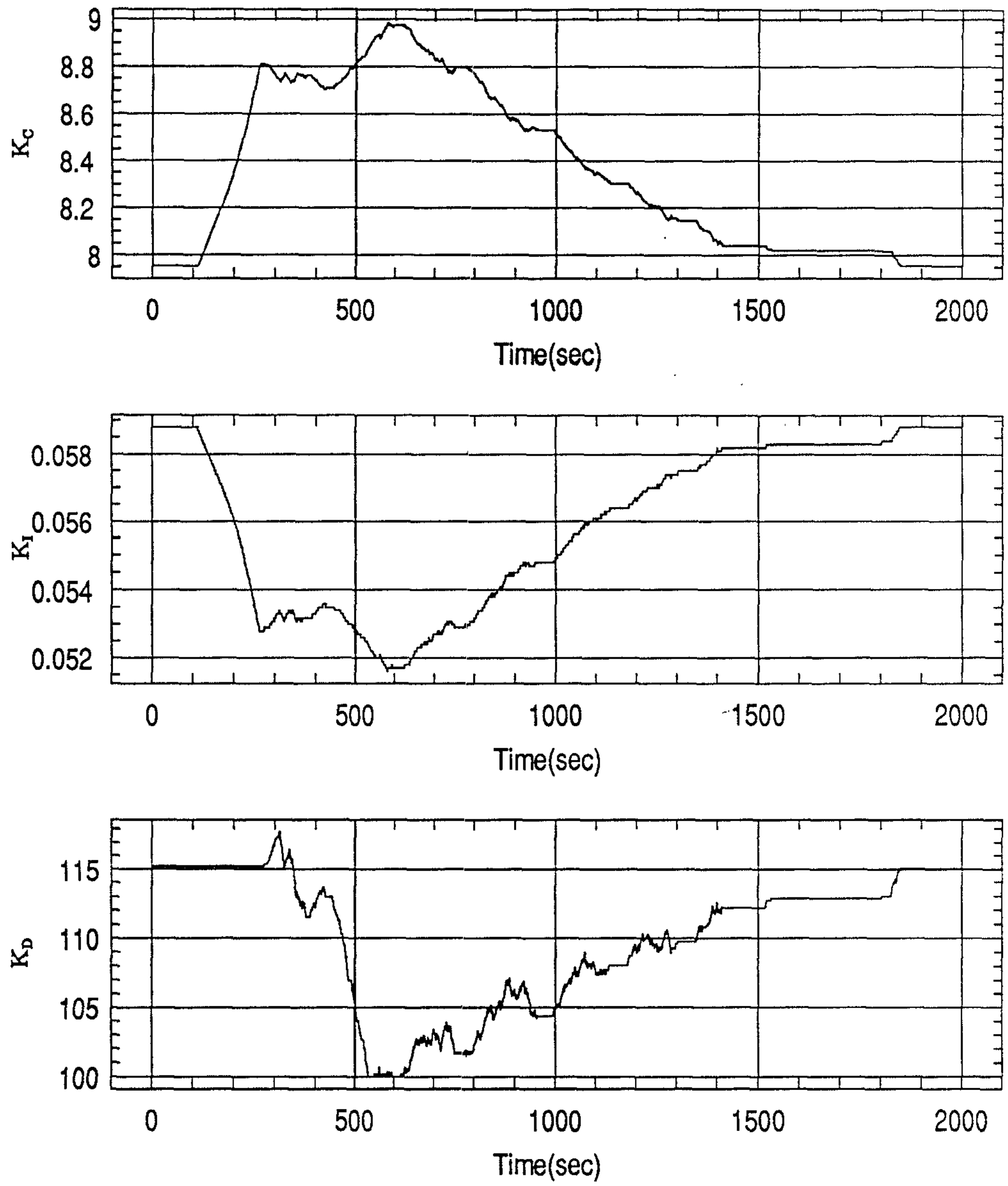

Figure 5.14: Separator(Initially Slow): Gain Scheduling During the Final Response

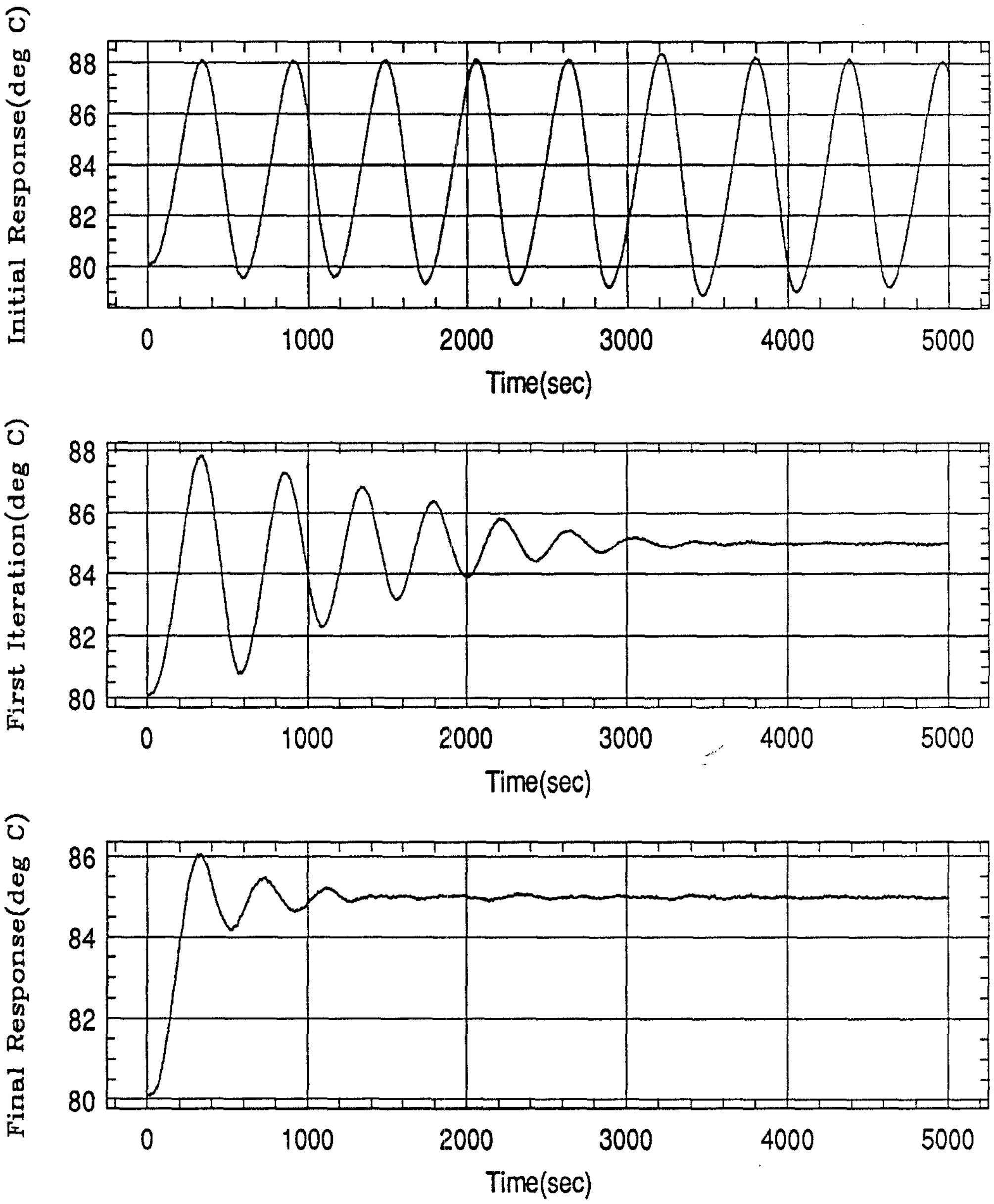

Figure 5.15: Separator: Oscillatory Initial Response (top), First Iteration Response (middle), Final Response (bottom)

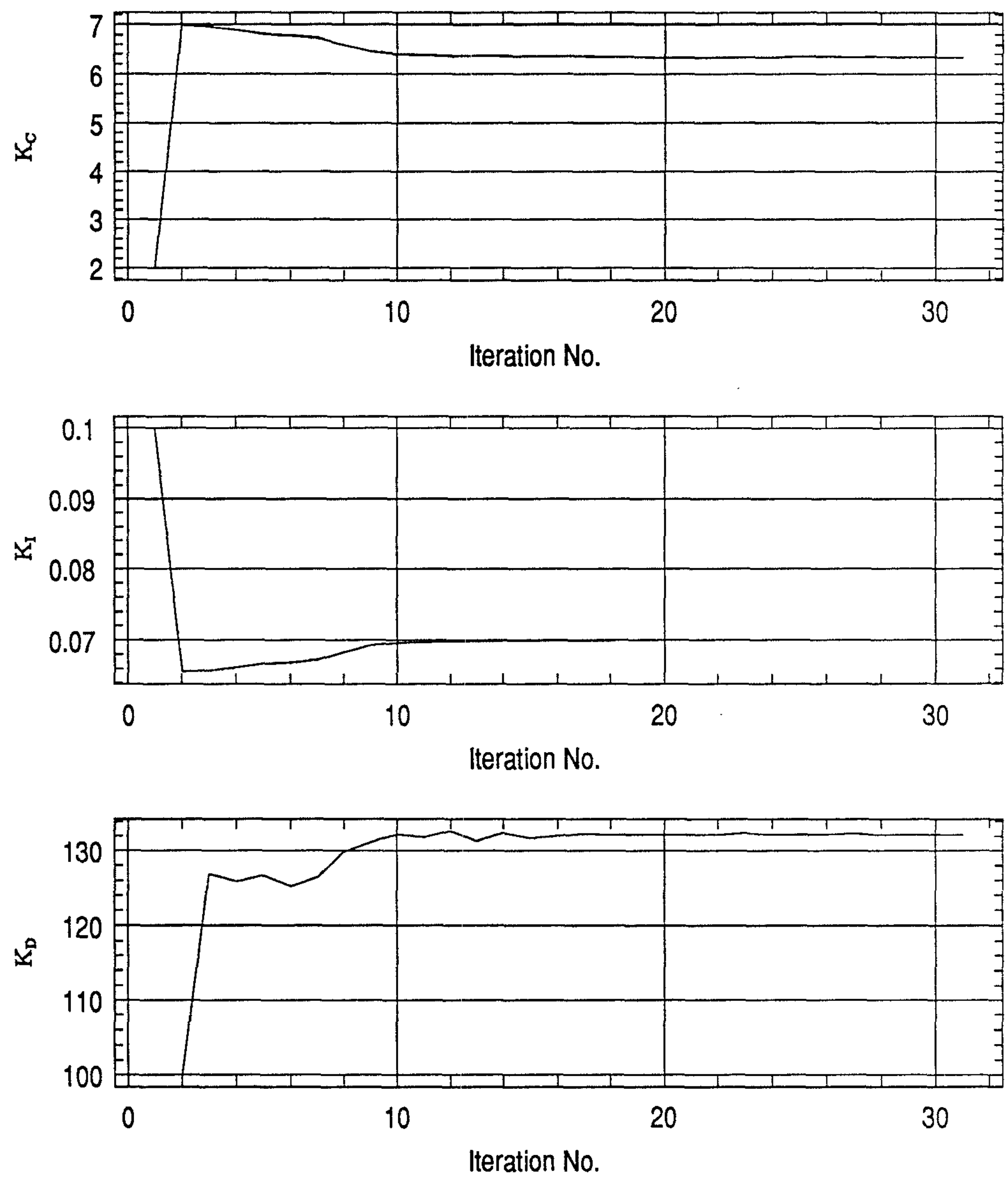

Figure 5.16: Separator(Oscillatory): Steady State Gains Versus Iteration Number

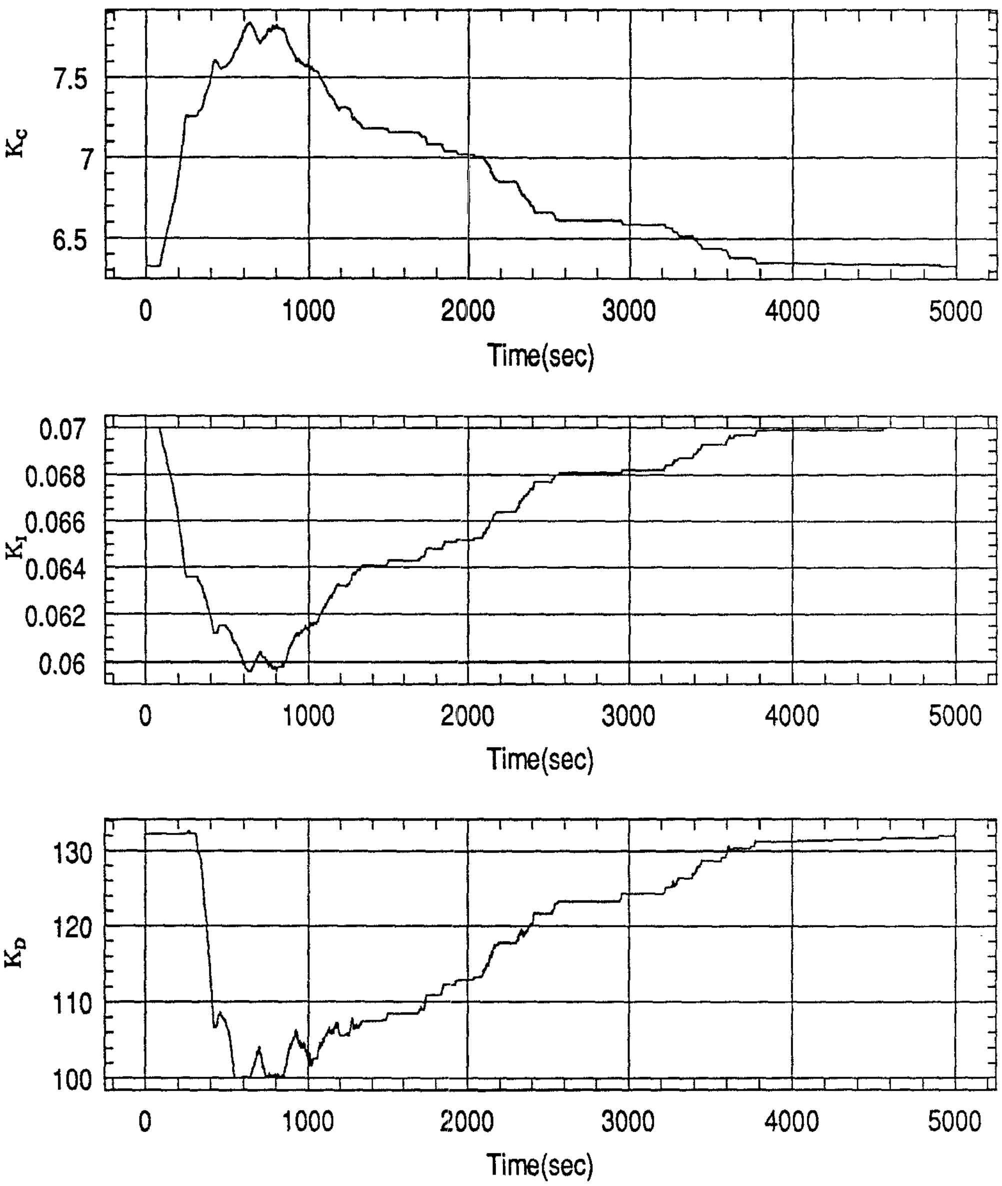

Figure 5.17: Separator(Oscillatory): Gain Scheduling During the Final Response

can be seen in the initial response shown in Figure 5.18. Figure 5.18 also shows the final response obtained after the gains have settled. It is seen that the rise time is again small. However this is obtained at the expense of a greater overshoot. This is to be expected, as the response is being forced to rise at its original rate , even though the capacity, or the time constant of the open loop system has been increased due to a greater amount of liquid. The plot of steady state gains with respect to iteration number is illustrated in Figure 5.19. This case is considered again in Section 5.4.

5.3 Third Order Plant

The plant considered has the following transfer function

$$P(s) = \frac{Y(s)}{U(s)} = \frac{0.0301}{(s+0.01)(s^2+10s+41)} \tag{5.2}$$

Here $\lambda_1 = -0.01$, $\lambda_{2,3} = -5 \pm j4$, and λ_1 is the dominant pole. The reference response (Figure 5.20) has $T_1 = 20$ seconds, and $T_2 = 250$ seconds. The initial PID parameters yield a very large rise time (Figure 5.20). The following parameters are chosen for the expert.

$\eta_1 = \eta_2 = 1$, $\eta_3 = 50$, $\rho_{K_C} = \rho_{K_D} = \rho_{K_I} = 0.005$, $K_{C_{max}} = 30$, $K_{C_{min}} = 0$, $K_{D_{max}} = 1500$, $K_{D_{min}} = 10$, $K_{I_{max}} = 1$, and $K_{I_{min}} = 0$. A set-point change from 0 to 10 is considered.

The final response after the application of the expert is shown in Figure

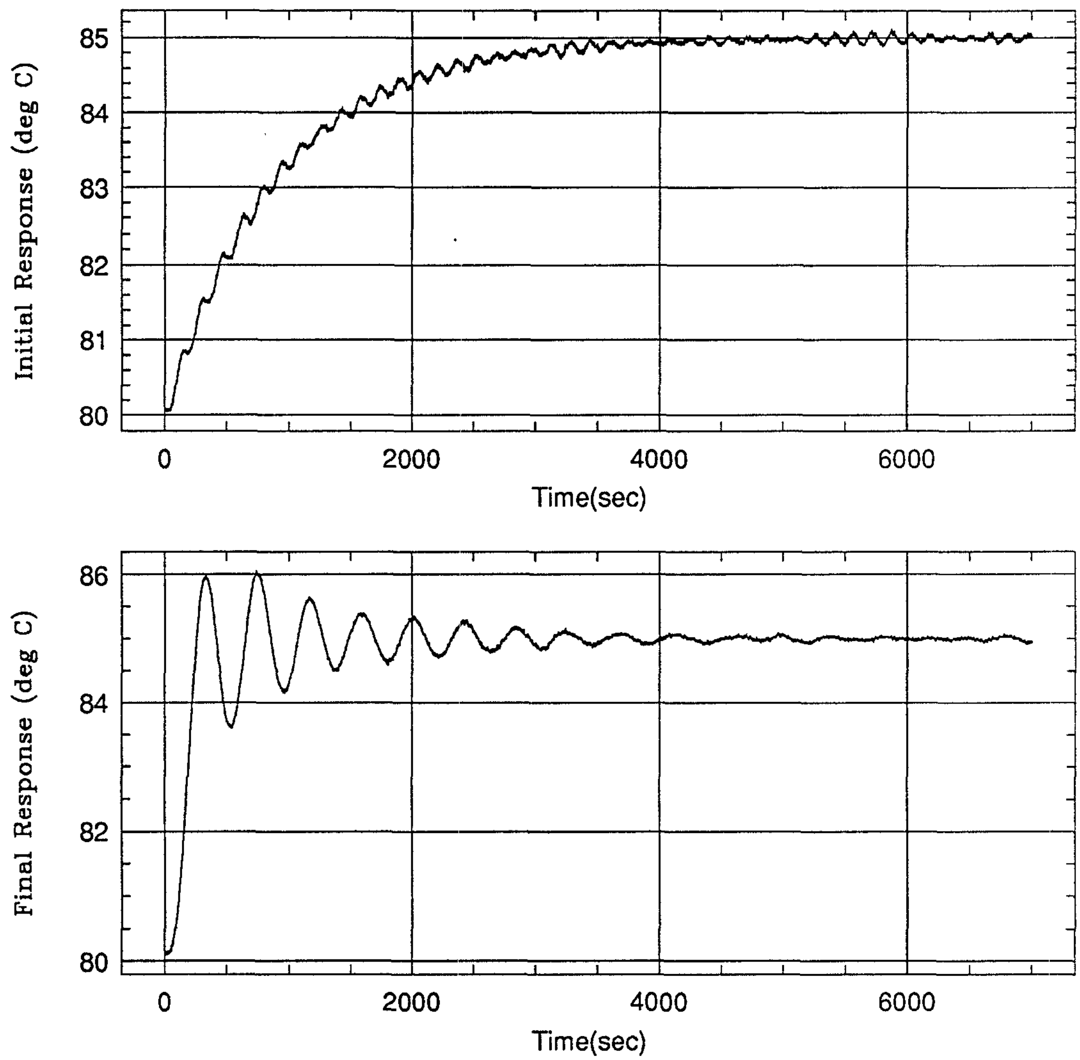

Figure 5.18: Separator(Liquid Level Change): Initial Response(top), Final Response(bottom)

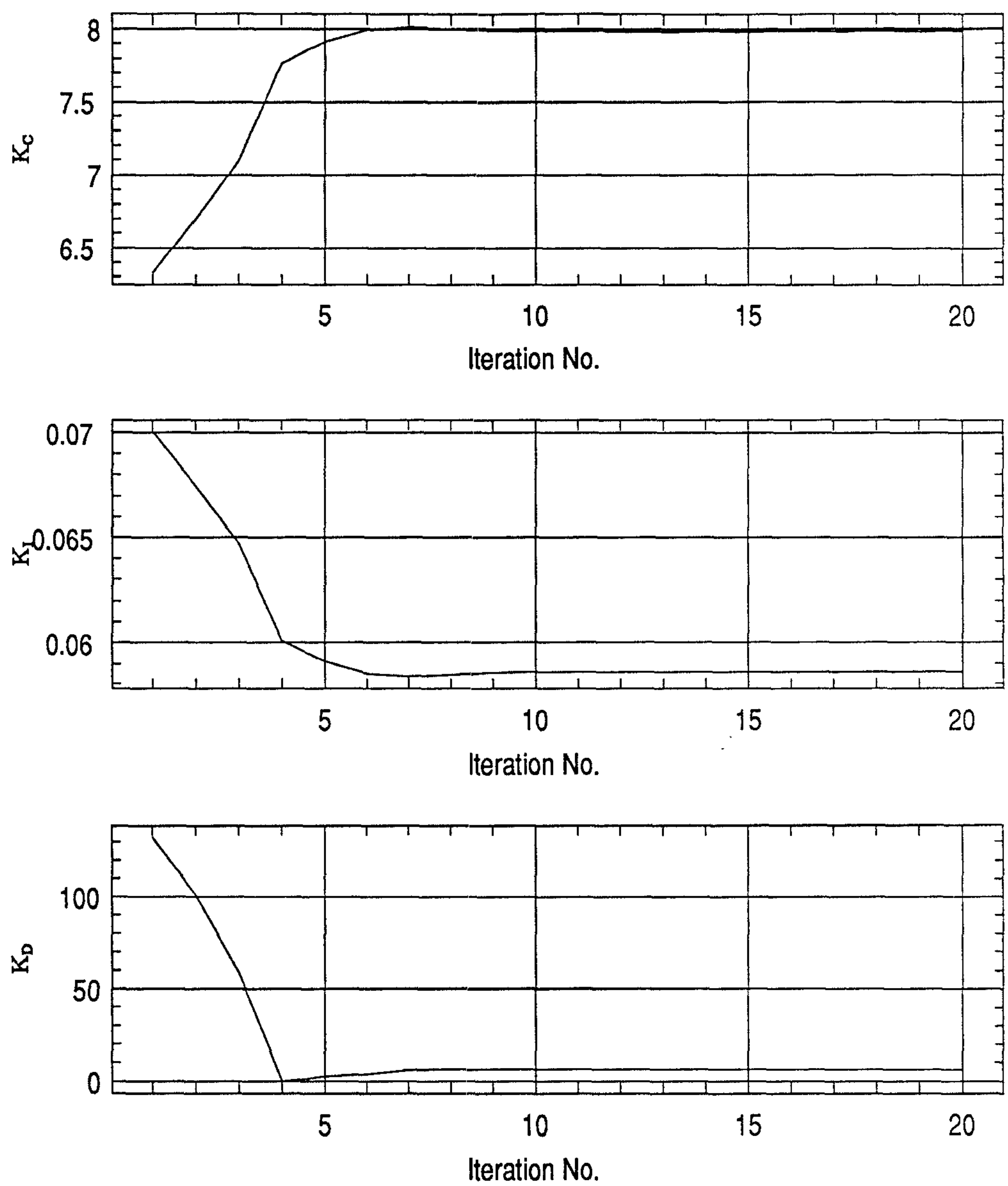

Figure 5.19: Separator(Liquid Level Change): Steady State Gains Versus Iteration Number

5.20. Figure 5.21 shows the variation in the steady state gains from iteration to iteration. It is seen that the expert successfully tunes the gains, and this supports the claim made in Section 3.4, concerning robustness of the portion of the root locus of interest with respect to unaccounted higher order poles.

5.4 Expert With Overshoot Control and Adaptive Scaling

In the case of seperator temperature control with a change in the liquid level, it is seen that the final response is highly oscillatory (Figure 5.18). This is because, an increase in the liquid level pushes the dominant pole towards the origin. Due to this the root locus also shifts, and this results in low damping, leading to a highly oscillatory response. The same system is considered again, however now the expert is augmented with the overshoot controller and adaptively modifies the frame 2 scaling factors. The maximum allowable overshoot is fixed at 10%. The final response obtained after the expert has tuned the gains is illustrated in Figure 5.22. It is observed that there is a dramatic improvement in the quality of the response obtained here as compared to that obtained by using the expert alone.

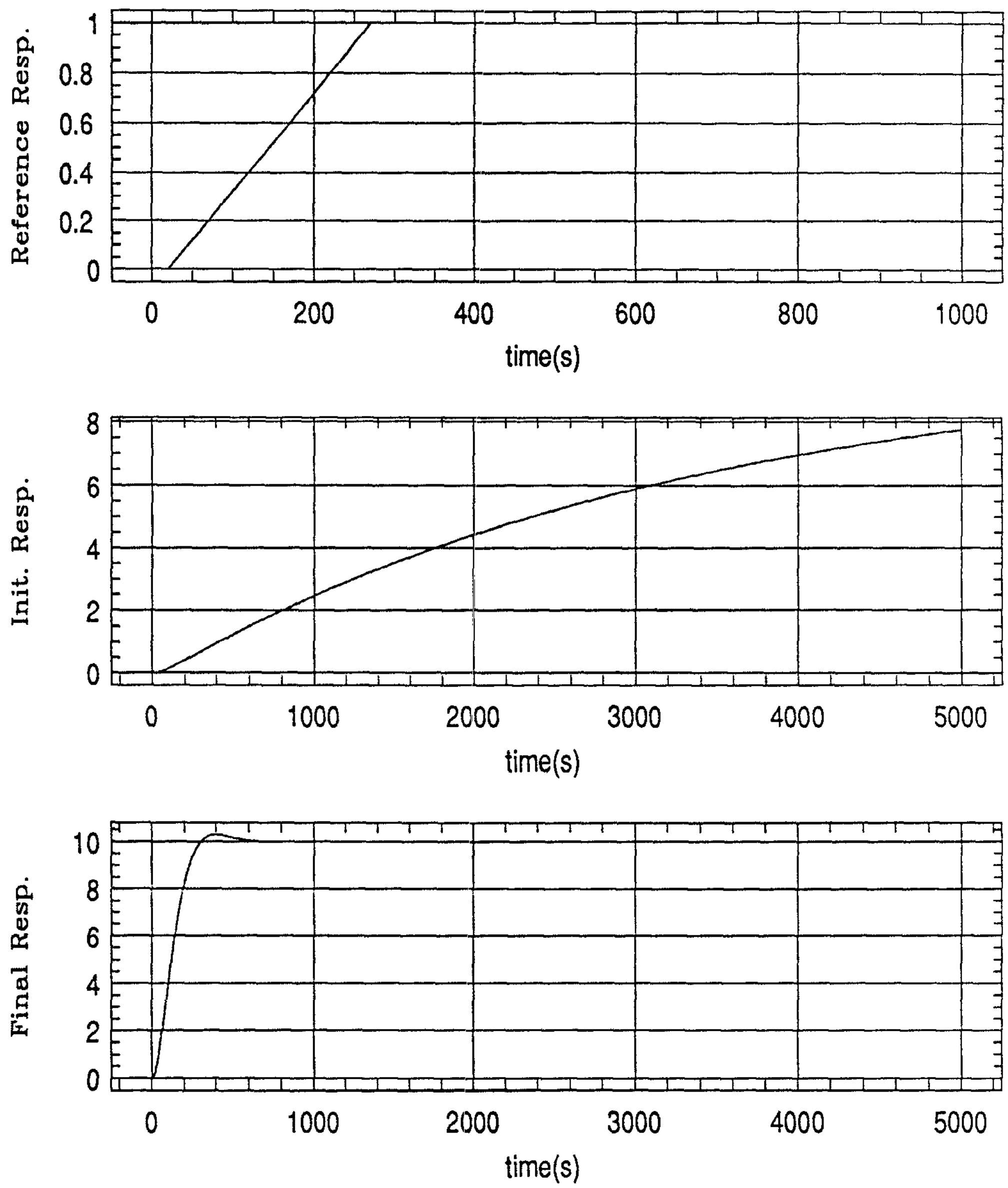

Figure 5.20: Third Order Plant: Reference Response (top), Initial Response (middle), and Final Response (bottom)

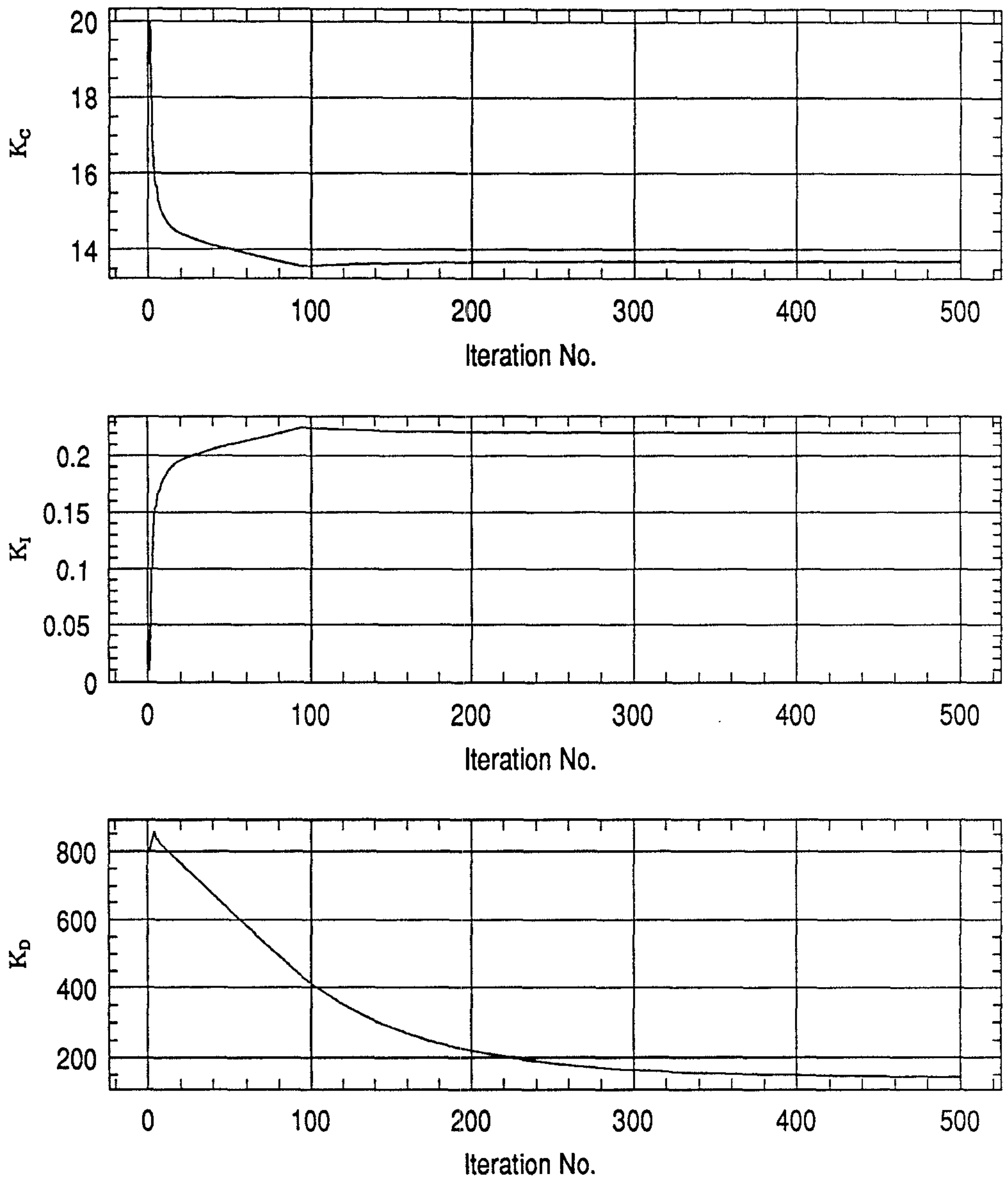

Figure 5.21: Third Order Plant: Steady State Gains Versus Iteration Number

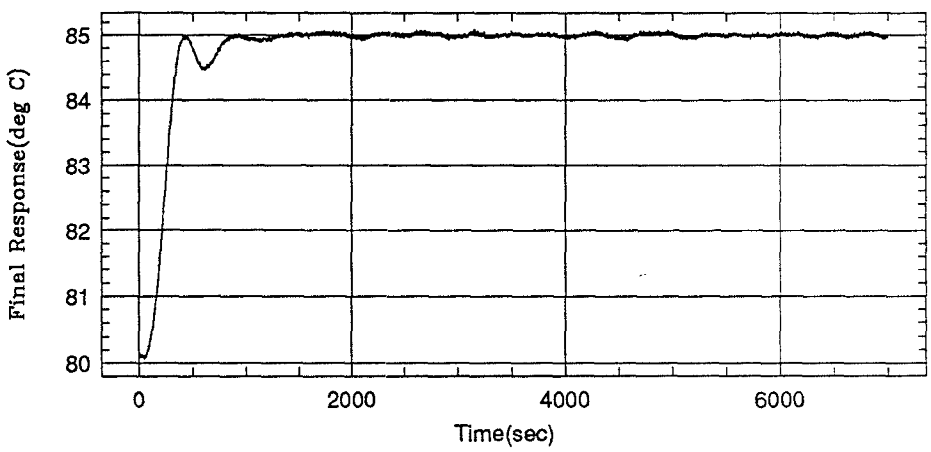

Figure 5.22: Seperator(Liquid Level Change): Final Response Obtained With Overshoot Control and Adaptive Scaling

Chapter 6

Conclusion

As seen in the applications discussed in Chapter 5, the expert is successful in tuning the gains of the PID controllers. The way the fuzzy rules have been formulated, it is seen that the derivative mode gain(K_D) is usually very small. For example in case of the separator, Cohen-Coon tuning [Coon, 1956] gives a derivative gain of 186, as compared to 115 and 132 obtained by using the expert. Smaller derivative gains are desirable as they imply less valve jitter in the presence of measurement noise.

Since many chemical control loops have plants which have a similar open loop characteristics as the cases discussed, the expert maybe applied to them for the tuning of their PID gains. Further flexibility maybe obtained by creating a *supervisor* for the expert. The performance improvement achieved by incorporating an overshoot controller and by using adaptive scaling have been demonstrated in Section 5.4.

In this thesis, a great amount of emphasis has been placed on the concept of manipulating the root locus and hence, the poles of the closed-loop system via movement of the controller zeroes. This approach could lead to a better means of improving the system response, rather than gain(N) variation (which is more common in the literature), especially since noise restricts the range over which the gain can be varied.

It is seen that the rule base presented in this thesis adequately tunes the gains. There is no claim made that modifications in the rule base will not result in a better performance. In fact, another rule base may result in a better performance by manipulating the zeroes in a different manner. A surprising fact is, that although the analysis presented in Appendix B only ensures that the rules manipulate the zeroes as desired for particular values of the controller gains, they seem to be able to compensate even if the gains are much smaller than those assumed. E.g. this is seen in the case of the second order plant, where the derivative gain(K_D) is almost zero, whereas its range is of a much greater magnitude.

Finally it can be said that the results obtained provide encouragement towards the goal of developing intelligent controllers to handle a class of systems. However, there is a strong need for the development of mathematical tools for the analysis of fuzzy systems. Without precise mathematical statements, the acceptance of such controllers in industry will remain doubtful. The results also demonstrate the need for developing methods for evaluating the performance of such intelligent controllers.

Appendix A

Controller Zeroes and Closed Loop Poles

This appendix considers the effect of the movement of the complex controller zeroes on the complex closed-loop poles. Attention is restricted to moving the poles and zeroes towards the imaginary axis, and away from the real axis. The closed loop transfer function is given by

$$G(s) = \frac{P(s)}{1 + C(s)P(s)} \tag{A.1}$$

where the closed loop poles have to satisfy

$$1 + C(s)P(s) = 0 \tag{A.2}$$

This reduces in the case of interest to

$$1 + \frac{K(s + z_1)(s + z_2)}{s(s + \lambda_1)(s + \lambda_2)} \tag{A.3}$$

where $-z_1$, $-z_2$ are the controller zeroes, $-\lambda_1$, $-\lambda_2$ are the plant poles and K is the plant gain. Now let $z_1 = \alpha + j\beta$ and $z_2 = \alpha - j\beta$. Hence equation A.3 reduces to

$$s^3 + (\lambda_1 + \lambda_2 + K)s^2 + (\lambda_1\lambda_2 + 2\alpha K)s + (\alpha^2 + \beta^2)K = 0 \tag{A.4}$$

The roots s_1, s_2 and s_3 of this equation have to satisfy

$$s_1 + s_2 + s_3 = -(\lambda_1 + \lambda_2 + K) \tag{A.5}$$

$$s_1 s_2 + s_2 s_3 + s_3 s_1 = \lambda_1\lambda_2 + 2\alpha K \tag{A.6}$$

$$s_1 s_2 s_3 = -(\alpha^2 + \beta^2)K \tag{A.7}$$

Let $f_i = \frac{ds_i}{d\alpha}$, i=1,2,3. Then differentiating A.5 - A.7 with respect to α one obtains

$$f_1 + f_2 + f_3 = 0 \tag{A.8}$$

$$s_1 f_2 + s_2 f_1 + s_2 f_3 + s_3 f_2 + s_1 f_3 + s_3 f_1 = 2K \tag{A.9}$$

$$s_1 s_3 f_2 + s_2 s_3 f_1 + s_1 s_2 f_3 = -2\alpha K \tag{A.10}$$

Writing it in matrix form gives

$$\begin{bmatrix} 1 & 1 & 1 \\ s_2 + s_3 & s_1 + s_3 & s_1 + s_2 \\ s_2 s_3 & s_1 s_3 & s_1 s_2 \end{bmatrix} \begin{bmatrix} f_1 \\ f_2 \\ f_3 \end{bmatrix} = \begin{bmatrix} 0 \\ 2K \\ -2\alpha K \end{bmatrix} \tag{A.11}$$

$\Rightarrow$

$$\begin{bmatrix} f_1 \\ f_2 \\ f_3 \end{bmatrix} = \frac{1}{\Delta} \begin{bmatrix} s_1^2(s_2 - s_3) & -s_1(s_2 - s_3) & s_2 - s_3 \\ s_2^2(s_3 - s_1) & -s_2(s_3 - s_1) & s_3 - s_1 \\ s_3^2(s_1 - s_2) & -s_3(s_1 - s_2) & s_1 - s_2 \end{bmatrix} \begin{bmatrix} 0 \\ 2K \\ -2\alpha K \end{bmatrix} \tag{A.12}$$

where $\Delta = s_1^2(s_2 - s_3) + s_2^2(s_3 - s_1) + s_3^2(s_1 - s_2)$. Let $\gamma = s_3$ be the real root. Hence one can write the other two roots as $s_1 = \lambda + j\omega$ and $s_2 = \lambda - j\omega$ where

$\lambda < 0$. Since the interest here is in the movement of the complex roots, it suffices to study only f_1. From equation A.12 one obtains

$$f_1 = \frac{-2Ks_1(s_2 - s_3) - 2\alpha K(s_2 - s_3)}{\Delta} \tag{A.13}$$

Substituting for the values of s_1, s_2 and s_3 one gets

$$f_1 = \frac{K(\gamma + \alpha)}{(\gamma - \lambda)^2 + \omega^2} + j\frac{K(\omega^2 - (\gamma - \lambda)(\lambda + \alpha))}{\omega((\gamma - \lambda)^2 + \omega^2)} \tag{A.14}$$

$\Rightarrow$

$$\frac{d\lambda}{d\alpha} = \frac{K(\gamma + \alpha)}{(\gamma - \lambda)^2 + \omega^2} \tag{A.15}$$

$$\frac{d\omega}{d\alpha} = \frac{K(\omega^2 - (\gamma - \lambda)(\lambda + \alpha))}{\omega((\gamma - \lambda)^2 + \omega^2)} \tag{A.16}$$

Now let $g_i = \frac{ds_i}{d\beta}$, i=1,2,3. Then differentiating equations A.5 - A.7 with respect to β one obtains

$$g_1 + g_2 + g_3 = 0 \tag{A.17}$$

$$s_1g_2 + s_2g_1 + s_2g_3 + s_3g_2 + s_1g_3 + s_3g_1 = 0 \tag{A.18}$$

$$s_1s_2g_2 + s_2s_3g_1 + s_1s_2g_3 = -2\beta K \tag{A.19}$$

Under similar assumptions one gets

$$g_1 = \frac{\beta K}{(\gamma - \lambda)^2 + \omega^2} - j\frac{\beta K(\gamma - \lambda)}{\omega((\gamma - \lambda)^2 + \omega^2)} \tag{A.20}$$

and hence

$$\frac{d\lambda}{d\beta} = \frac{\beta K}{(\gamma - \lambda)^2 + \omega^2} \tag{A.21}$$

$$\frac{d\omega}{d\beta} = \frac{-\beta K(\gamma - \lambda)}{\omega((\gamma - \lambda)^2 + \omega^2)} \tag{A.22}$$

Under the assumption that $\mid \gamma \mid > \mid \lambda \mid, \mid \alpha \mid$ one gets from equations A.15, A.21 and A.22

$$\frac{d\lambda}{d\alpha} < 0 \quad , \frac{d\lambda}{d\beta} > 0 \quad , and \quad \frac{dw}{d\beta} > 0. \tag{A.23}$$

Hence moving the controller zeroes towards the imaginary axis and away from the real axis pushes the closed loop poles towards the imaginary axis. Now lets consider equation A.16. Setting $\alpha = 0$ (i.e. zeroes on the imaginary axis), gives

$$\frac{d\omega}{d\alpha} = \frac{K(\omega^2 - \lambda(\gamma - \lambda))}{\omega((\gamma - \lambda)^2 + \omega^2)} \tag{A.24}$$

So if $\omega^2 + \lambda^2 < \lambda\gamma$ (*) $\Rightarrow$

$$\frac{d\omega}{d\alpha} < 0. \tag{A.25}$$

Hence if the above condition(*) holds then by the continuity of $\frac{d\omega}{d\alpha}$ there exists a region near the imaginary axis where A.25 is satisfied. Hence if the zeroes are sufficiently close to the imaginary axis then the poles follow the zeroes. However in practice, the extent of the region where A.25 holds is not known. What is known however, is that such a region does exist and is near the origin. Since the aim here is to influence ω using both α and $beta$, and the sign of $\frac{d\omega}{d\beta}$ is known to be greater than zero, one makes $\mid \Delta\beta \mid \gg \mid \Delta\alpha \mid$. A positive sign on $\frac{d\omega}{d\alpha}$ is advantageous as, if the poles are too far away from the origin, then moving the zeroes away from the real axis causes ω to increase. Too large a value of ω drives all the derivative terms to zero and ultimately the influence of the zeroes on the poles will be negligible. $\frac{d\omega}{d\alpha}$ counters this growth of ω .

Once the zeroes are close to the imaginary axis, change in α is small, since it can only reach zero in the limit. Hence now the zero-pole movement is determined by β, whose influence on λ and ω is known.

Note that in the first order plant case, one can set $\gamma \to \infty$. Hence condition (*) holds trivially.

Appendix B

Analysis of Fuzzy Rules

This appendix presents an order of magnitude analysis of the fuzzy rules presented in Table 3.1 and Table 3.2. The analysis is carried out under certain assumptions. These are

1. The PID gains are of the same order of magnitude as their respective ranges (R_{K_C}, R_{K_D} and R_{K_I}).

2. The output scaling factors are approximately the same i.e. $\rho_{K_C} \approx \rho_{K_D} \approx \rho_{K_I}$.

3. The controller zeroes are complex.

The ranges are defined as follows

$$R_{K_C} = K_{C_{max}} - K_{C_{min}}$$

$$R_{K_D} = K_{D_{max}} - K_{D_{min}}$$

$$R_{K_I} = K_{I_{max}} - K_{I_{min}}$$

Let the controller zero z_1 be given by

$$z_1 = \alpha + j\beta \tag{B.1}$$

where

$$\alpha = \frac{-K_C}{2K_D} \tag{B.2}$$

and

$$\beta = \frac{K_C}{2K_D}\sqrt{\frac{4K_D K_I}{K_C^2} - 1} \tag{B.3}$$

Differentiating equation B.2 one gets

$$\Delta\alpha \approx \frac{-1}{2K_D}\Delta K_C + \frac{K_C}{2K_D^2}\Delta K_D \tag{B.4}$$

$\Rightarrow$

$$\Delta\alpha \approx \frac{1}{2K_D}(\frac{K_C}{K_D}\rho_{K_D} R_{K_D}\delta_{K_D} - \rho_{K_C} R_{K_C}\delta_{K_C}) \tag{B.5}$$

By the assumptions, $\frac{K_C R_{K_D}}{K_D} \approx R_{K_C}$, and $\rho_{K_D} \approx \rho_{K_C} = \rho$. Hence one has

$$\Delta\alpha \approx \frac{\rho R_{K_C}(\delta_{K_D} - \delta_{K_C})}{2K_D} \tag{B.6}$$

Differentiating equation B.3 one gets

$$\Delta\beta \approx \{[\frac{1}{2K_D}(\frac{4K_D K_I}{K_C^2} - 1) - \frac{2K_I}{K_C^2}]\Delta K_C + [\frac{-K_C}{2K_D^2}(\frac{4K_D K_I}{K_C^2} - 1) + \frac{K_I}{K_D K_C}]\Delta K_D$$
$$+ \frac{1}{K_C}\Delta K_I\}\frac{1}{\sqrt{\frac{4K_D K_I}{K_C^2} - 1}} \tag{B.7}$$

$\Rightarrow$

$$\Delta\beta \approx \{\frac{-1}{2K_D}\Delta K_C + \frac{1}{K_P}\Delta K_I + (\frac{K_C}{2K_D^2} - \frac{K_I}{K_C K_D})\Delta K_D\}\frac{1}{\sqrt{\frac{4K_D K_I}{K_C^2} - 1}} \tag{B.8}$$

$\Rightarrow$

$\Delta\beta \approx$

$$\{\frac{-\rho_{K_C} R_{K_C}}{2K_D}\delta_{K_C} + \frac{\rho_{K_D} R_{K_D} K_C}{2K_D^2}\delta_{K_D} + \frac{\rho_{K_I} R_{K_I}}{K_C}\delta_{K_I} - \frac{K_I \rho_{K_D} R_{K_D}}{K_C K_D}\delta_{K_D}\}\frac{1}{\sqrt{\frac{4K_D K_I}{K_C^2} - 1}} \tag{B.9}$$

By the assumptions, $\frac{K_C}{K_D} R_{K_D} \approx R_{K_C}$, $\frac{K_I}{K_D} R_{K_D} \approx R_{K_I}$, and $\rho_{K_C} \approx \rho_{K_I} \approx \rho_{K_D} = \rho$. Hence one has

$$\Delta\beta \approx \frac{1}{\sqrt{\frac{4K_D K_I}{K_C^2} - 1}}\{\frac{\rho R_{K_C}}{2K_D}(\delta_{K_D} - \delta_{K_C}) + \frac{\rho R_{K_I}}{K_C}(\delta_{K_I} - \delta_{K_D})\} \tag{B.10}$$

Frame 1: If $e_1\prime(t)$ *Positive Small* or *Positive Medium* then one has $\delta_{K_D} = 0$, $\delta_{K_I} > 0$ and $\delta_{K_C} < 0$, with $|\delta_{K_C}| \approx |\delta_{K_I}|$. $\Rightarrow \Delta\alpha > 0$, and $\Delta\beta > 0$.

If on the other hand $e_1\prime(t)$ is *Positive Large* then $\delta_{K_C} < 0 < \delta_{K_D} < \delta_{K_I}$. $\Rightarrow \Delta\alpha > 0$, and $\Delta\beta > 0$. It is also clear that $|\Delta\beta| > |\Delta\alpha|$ as $\Delta\beta$ can be written as

$$\Delta\beta \approx \Delta\alpha + \frac{\rho R_{K_I}}{K_C}(\delta_{K_I} - \delta_{K_D}) \tag{B.11}$$

and $\frac{\rho R_{K_I}}{K_C}(\delta_{K_I} - \delta_{K_D})$ is always the same sign as $\Delta\alpha$ and $\Delta\beta$. Hence the zeroes move as desired.

Frame 2: If $e_2\prime(t) \neq$ *Small* or $\frac{de_2\prime(t)}{dt} \neq$ *Zero* then $\delta_{K_D} < 0$, $\delta_{K_C} > 0$, and $\delta_{K_I} < 0$ with $|\delta_{K_C}| \approx |\delta_{K_I}| < |\delta_{K_D}|$. $\Rightarrow \Delta\alpha < 0$, and $\Delta\beta \approx 0$ assuming $\frac{R_{K_C}}{2K_D} \approx \frac{R_{K_I}}{K_C}$.

If $e_2\prime(t)$ is *Small* and $\frac{de_2\prime(t)}{dt}$ is *Zero* then $\delta_{K_D} > 0$, $\delta_{K_C} < 0$, and $\delta_{K_I} > 0$ with $|\delta_{K_D}|$

$\approx |\delta_{K_C}| \approx |\delta_{K_I}|$. $\Rightarrow \Delta\alpha > 0$, and $\Delta\beta > 0$. Hence once again the zeroes move as required.

Thus it is seen that under the given assumptions, the fuzzy rules manipulate the zeroes as desired.

Bibliography

[Åström, 1991] Åström, K. J., "Directions in intelligent control", IFAC Intelligent Tuning and Adaptive Control, Singapore, 1991, pp. 1-9.

[Åström and McAvoy, 1992] Åström, K. J. and T. J. McAvoy, "Intelligent control", Journal of Process Control, Vol. 2, 1992, pp. 115-126.

[Bernard, 1988] Bernard, J., "Use of rule-based system for process control", IEEE Control Systems Magazine, Oct. 1988.

[Bohl and McAvoy, 1976] Bohl, A. H. and T. J. McAvoy, "Linear feedback vs. time optimal control, 1. The servo problem", Ind. Eng. Chem. Process Des. Dev., Vol. 15, No. 1, 1976, pp. 24-29.

[Chiu *et al.*, 1990] Chiu, S., S. Chand, D. Moore and A. Chowdhary, "Fuzzy logic control of roll and moment for a flexible wing aircraft", IEEE Control Systems Magazine, June 1991, pp. 42-48.

[Coon, 1956] Coon, G. A., "How to find controller settings from process characteristics", Control Engineering, Vol. 3, No. 5, 1956, pp. 66-76.

[Holmblad and Østergaard, 1981] Holmblad, L. P. and J. Østergaard, "Control of cement kiln by fuzzy logic", F. L. Smidth Review, Vol. 67, Copenhagen, Denmark, 1981, pp. 3-11.

[Koivo and Tanttu, 1991] Koivo, H. N. and J. T. Tanttu, "Tuning of PID controllers: survey of SISO and MIMO techniques", IFAC Intelligent Tuning and Adaptive Control, Singapore, 1991, pp. 75-80.

[Kosko, 1990] Kosko, Bart, "Neural networks and fuzzy systems", Prentice-Hall, Englewood Cliffs, NJ, 1990.

[Kuo, 1991] Kuo, B. C.,"Automatic control systems (6th edition)", Prentice-Hall, Englewood Cliffs, NJ, 1991.

[Latour *et al.*, 1967] Latour, P. R., L. B. Koppel and D. R. Coughanour, "Time optimal control of chemical processes for set point changes", Ind. Eng. Chem. Process Des. Dev., Vol. 7, No. 3, 1967, pp. 345-353.

[Oldenburg and Sartorius, 1948] Oldenburg, R. C. and H. Sartorius, "Dynamics of automatic controls", ASME, NY, 1948.

[Pedrycz, 1989] Pedrycz, W., "Fuzzy control and fuzzy systems", Research Studies Press, Somerset, England, 1989.

[Self, 1990] Self, Kevin, "Designing with fuzzy logic", IEEE Spectrum, Nov. 1990.

[Sugeno, 1985] Sugeno, M. (Ed), "Industrial applications of fuzzy control", North-Holland, Amsterdam, The Neatherlands, 1985.

[van der Rhee *et al.*, 1990] van der Rhee, F., H. R. van Nauta Lemke and J. G. Dijkman, "Knowledge based fuzzy modeling of systems", 11th IFAC World Congress, Tallinn, Estonia, 1990.

[Vogel and Downs, 1990] Vogel, E. and J. Downs, "A plant-wide industrial process control problem", paper 24a, Chicago, IL, Nov. 1990.

[Zadeh, 1968] Zadeh, L. A., "Fuzzy Algorithms", Information and Control, Dec. 1968, pp. 94-102.

[Zadeh, 1973] Zadeh, L. A., "Outline of a new approach to the analysis of complex systems and decision processes", IEEE Trans. Syst., Man, Cybern., vol. SMC-3, No. 1, 1973, pp. 28-44.

[Zadeh, 1988] Zadeh, L. A., "Fuzzy logic", IEEE Computer, April, 1988, pp. 83-93.